PALEOINTENSITY OF THE ALLENDE CARBONACEOUS CHONDRITE

Takesi NAGATA and Minoru FUNAKI

National Institute of Polar Research, 9–10, Kaga 1-chome, Itabashi-ku, Tokyo 173

Abstract: The natural remanent magnetization (NRM) of the Allende carbonaceous chondrite appears to be much more complicated than interpretations given by previous works (*e.g.* BUTLER: Earth Planet. Sci. Lett., **17**, 23, 1972; BANERJEE and HARGRAVES: Earth Planet. Sci. Lett; **17**, 110, 1972; LANOIX *et al.*: Geophys. Res. Lett., **5**, 73, 1978; LANOIX *et al.*: Lunar Planet. Sci. IX, 630, 1978; NAGATA: Phys. Earth Planet. Inter., **20**, 324, 1979; SUGIURA *et al.*: Phys. Earth Planet. Inter., **20**, 342, 1979) as already pointed out by WASILEWSKI and SARALKER (Proc. Lunar Planet. Sci. Conf., 12B, 1217, 1981). The ferromagnetic and/or ferrimagnetic constituents in the Allende are Ni-rich taenite, pyrrhotite and magnetite, among which taenite is most dominant in spontaneous magnetization intensity.

NRM of the bulk specimen is uniform and very stable in AF-demagnetization test. NRM of matrix also is as stable as that of the bulk specimen, whereas NRM of most chondrules is either unstable or faint compared with that of matrix. The NRM intensity of bulk specimen is almost same as that of matrix specimen.

NRMs of the bulk and matrix specimens can be thermally demagnetized almost completely by heating to about 320°C. Their thermal demagnetization curves well resemble the thermomagnetic curve of ferrimagnetic pyrrhotite. However, the thermal demagnetization curves of chondrules having unstable NRM consist of a component thermally demagnetized by about 320°C and the other component thermally demagnetized by about 580°C. It is concluded from these results that the stable and uniform NRM of the Allende chondrite is mostly due to the stable NRM of matrix.

Experimental results of acquisition of the partial thermoremanent magnetization (PTRM) show that these specimens can acquire PTRM in a temperature range up to about 620°C, the largest PTRM acquisition rate taking place in a range of 500–600°C. It may be provisionally concluded therefore that the Allende NRM was acquired as PTRM during a course of cooling from about 320°C in the presence of a magnetic field or as the chemical remanent magnetization (CRM) of ferrimagnetic pyrrhotite during a formation process of ferrimagnetic pyrrhotite from iron sulfides at temperatures below 320°C.

Results of Königisberger-Thellier experiments of a number of bulk and matrix specimens and of a chondrule having stable NRM, on an assumption that NRM is PTRM acquired during a course of cooling from about 320°C in the presence of a magnetic field (F_p), lead to a conclusion that the paleointensity of the Allende chondrite is given by F_p=(1–3) Oe.

1. Introduction

In a review paper of magnetism and paleomagnetism of meteorites (NAGATA, 1979a), significance of the paleomagnetic intensity derived from the natural remanent magnetization (NRM) of Allende C3 chondrite was emphasized, because NRM of the Allende is extremely stable and the mineralogical composition of ferromagnetic constituents in this C3 chondrite appeared to be relatively simple so that an elevation of temperature of this chondrite up to their Curie point may result in only little alteration of their magnetic characteristics. The NRM of the Allende has been studied by several investigators with the Königisberger-Thellier method on an assumption that the acquisition process of NRM is the thermoremanent magnetization (TRM).

In the study of BANERJEE and HARGRAVES (1972), a linear relationship between NRM-lost and TRM-gained holds for a temperature range lower than 130°C, and the paleointensity (F_p) is determined as $F_p=(1.09\pm0.08)$ Oe. In BUTLER's work (1972), the upper limit temperature (T_0) for the linear relationship is 150°C and $F_p=(1.11\pm 0.14)$ Oe. However, the paleointensity values represent a magnetic field, in which this chondrite was cooled from T_0, whereas NRM corresponding to the cooling temperature range is only about 1/3 or less of the total NRM in both Butler's and Banerjee-Hargraves' experiments. On the other hand, LANOIX *et al.* (1978a, b) obtained large paleointensity values (around 7 Oe) on individual chondrules from the Allende using a modified Thellier method. Then, SUGIURA *et al.* (1979) re-examined NRM of individual chondrules from the Allende in more detail, concluding that NRM of the chondrules consist of at least two components of TRM; one is a high-temperature component which was acquired when the individual chondrules were cooled through Curie point and before they were assembled into the Allende meteorite and the other is a low-temperature component which was probably acquired in a field of about 1 Oe when the meteorite experienced thermal metamorphism or during the assembly of the meteorite.

In earlier studies as well as in these recent studies of magnetic properties of the Allende chondrite, the main Curie point of the saturation magnetization *vs.* temperature curve is at 580–620°C (*e.g.* NAGATA, 1979a), suggesting that the main ferromagnetic constituent in the Allende is taenite and/or magnetite. The composition and structure of opaque minerals (including ferromagnetic minerals) in the Allende have been clarified in detail by HAGGERTY and MCMAHON (1979). According to these investigators, opaque minerals in chondrules in the Allende are magnetite-sulfide-metal complexes which are classified into four major assemblages, *i.e.* (a) magnetite + NiFe metal, (b) magnetite + troilite + NiFe metal, (c) magnetite + troilite + pentlandite + NiFe metal, and (d) troilite ± pentlandite. NiFe metals are ferromagnetic and magnetite is ferrimagnetic. It seems possible further that some portions of both troilite and pentlandite have the composition and structure of ferrimagnetic pyrrhotite. Actually, WASILEWSKI and SARALKER (1981) have detected Curie point of pyrrhotite (320°C) in the thermomagnetic curves of chondrules from the Allende, which contain only iron sulfides and practically no magnetite and no Fe-Ni metal. Another significant key point found by these investigators would be that magnetically stable chondrules contain only iron sulfides, whereas magnetically unstable chondrules contain metal + magnetite + iron sulfides aggregates, where a criterion of magnetic stability is defined by the stability of NRM (I_n) and the saturated isothermal remanent magnetization (I_R) against the AF-demagnetization test.

On the basis of these experimental data, WASILEWSKI and SARALKER (1981) have suggested that a sulfidation process is probably responsible for the observed stable NRM of the bulk Allende chondrite, though a possible mechanism of an acquisition of the stable remanent magnetization by the iron sulfide phase (represented by pyrrhotite) has not been suggested. Both SUGIURA *et al.* (1979) and WASILEWSKI and SARALKER (1981) were concerned moslty with the magnetic properties and NRMs of individual chondrules of the Allende, though SUGIURA *et al.* examined those of a few samples of its matrix and white inclusion too.

At the present stage of studies of the magnetic properties and NRM of the Allende, therefore, it may be desirable to re-examine the bulk sample as well as chondrule and matrix of the Allende chondrite by taking into consideration the observed particular compositions of ferromagnetic (or ferrimagnetic) minerals in this chondrite. In the present study, the opaque magnetic constituents are re-examined for the Allende chondrite specimens before their magnetic properties are measured. The main interest of the present study is, however, concerned with NRM and the most probable paleointensity of the Allende chondrite.

2. Instrumentation

The magnetic hysteresis curves at various temperatures and the thermomagnetic curves of meteorite samples are measured by use of a vibration magnetometer, while the intensity and direction of remanent magnetizations at various stages are measured by a cryogenic magnetometer. Only a remark to be made is that any heating procedure of a meteorite sample above room temperature except the case of thermomagnetic measurement is carried out using the Taylor's method (TAYLOR, 1979) in order to minimize possible chemical alteration of the examined specimen at elevated temperatures. In practice, a meteoritic sample to be examined is packed by silica wool in an end of a 210 mm long tube made of hard glass or silica, whereas metallic Ti powders are packed by silica wool in the other end of tube; and after evacuating down to 10^{-4} Torr, the tube is sealed.

3. Opaque Minerals in the Allende Magnetite-Sulfide-Metal Complexes

The composition and structure of opaque minerals in chondrules of the Allende have been studied in fair detail by HAGGERTY and MCMAHON (1979) and the thermomagnetic characteristics of several chondrules selected from the Allende have been examined by WASILEWSKI and SARALKER (1981). In the present study, the composition and structure of opaque minerals of both chondrules and matrix are examined in order to confirm the ferromagnetic (or ferrimagnetic) constituents in the Allende specimen, the magnetic properties and the natural remanent magnetization of which are directly studied for paleomagnetic research purpose.

The sections of several parts of the Allende samples for magnetic measurements are examined with a reflection microscope for identifying opaque minerals and with EPMA for evaluating their chemical compositions. As shown in Fig. 1, for example, pentlandite is abundant, troilite and magnetite are common, and Fe-Ni metallic grains are often observed in both chondrules and matrix of the Allende. Grain sizes of pentlandite and troilite are relatively large, being smaller than 500 μm, whereas those of magnetite and Fe-Ni metal are very small, being less than 20 μm in their mean diameters.

In Table 1, chemical compositions of troilite (Tr), pentlandite (Pe) and taenite (Fe-Ni) in the matrix are summarized. The chemical compositions of these opaque minerals in the matrix are substantially same as those of respective minerlas in chondrules in the Allende reported by HAGGERTY and MCMAHON (1979). In Table 2, the chemical compositions of magnetite grains in a chondrule and matrix are given, where FeO and Fe_2O_3 are calculated assuming that Fe_3O_4 is stoichiometric. For comparison, average values of 5 measurements of the chemical compositions of magnetite in chondrules of the Allende reported by HAGGERTY and MCMAHON are shown in the same

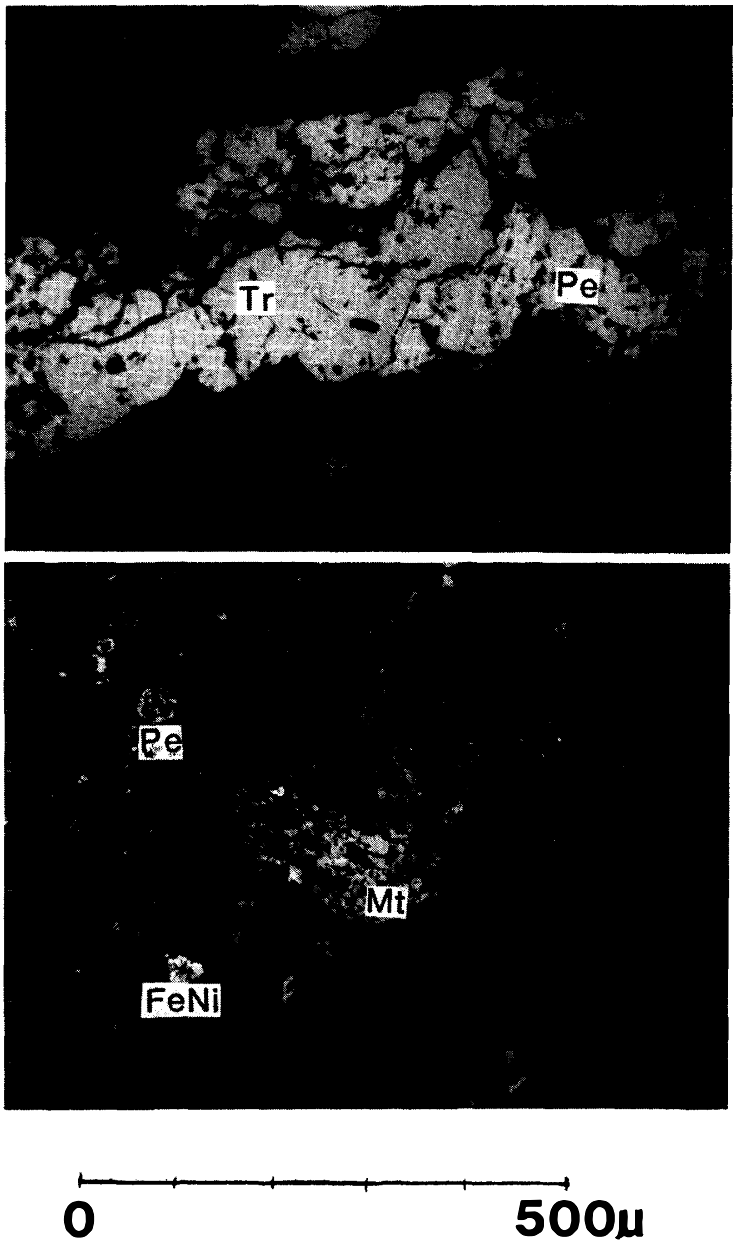

Fig. 1. Troilite (Tr), pentlandite (Pe), magnetite (Mt) and taenite (Fe-Ni) in the Allende matrix.

Table 1. Chemical composition of metal and sulfide grains in the matrix of the Allende (wt %).

	1–1 Tr	1–2 Tr	2–1 Pe	2–2 Pe	3 Pe	4 Pe	5 Tr	6 Fe-Ni	7 Fe-Ni
Fe	63.40	63.57	45.36	46.16	45.07	46.15	61.54	29.35	28.95
Co	0.050	0.00	1.71	1.74	0.99	0.85	0.00	1.99	1.96
Ni	0.00	0.055	18.16	17.88	21.25	18.84	0.008	67.92	67.51
S	36.65	35.38	33.33	33.31	33.83	33.11	36.26	0.00	0.040
Total	100.10	99.005	98.56	99.09	101.14	98.95	97.808	99.26	98.46

(1–1) and (1–2) are 2 different points in a grain of troilite.
(2–1) and (2–2) are 2 different points in a grain of pentlandite.

Table 2. Chemical composition of magnetite grains (wt %).

	Magnetite in chondrule	Magnetite in matrix		Magnetite in chondrules (HAGGERTY and MCMAHON)
	1	2–1	2–2	
SiO_2	0.23	3.09	4.74	—
TiO_2	0.00	0.15	0.072	0.05 ± 0.01
Al_2O_3	1.60	4.17	2.20	1.14 ± 0.19
Cr_2O_3	1.14	1.17	0.29	1.81 ± 0.10
Fe_2O_3*	66.17	53.41	53.05	65.83 ± 0.28
FeO*	29.77	24.03	23.87	30.12 ± 0.12
MgO	0.26	5.46	5.29	0.67 ± 0.06
MnO	0.00	0.092	0.051	0.03 ± 0.00
NiO	0.070	2.45	3.15	0.03 ± 0.03
CaO	0.66	0.60	1.03	—
Na_2O	0.15	0.039	0.25	—
K_2O	0.00	0.008	0.040	—
P_2O_5	0.72	0.00	0.019	—
Tatal	100.77	94.67	94.05	99.68

* It is assumed that $Fe_3O_4=FeO+Fe_2O_3$ is stoichiometric for the Fe oxide.

table. It seems likely that the composition of chondrule magnetite obtained in the present analysis is nearly same as that obtained by HAGGERTY and MCMAHON, whereas the matrix magnetites are considerably richer in MgO and NiO compared with the chondrule magnetites. This result may suggest that the magnetite grains in matrix contain a considerable amount of silicate phases as directly indicated by the observed presence of SiO_2 in the matrix magnetite grains. A considerably less content of Fe_3O_4 and a considerable defect of the total mass in the matrix magnetites may further suggest that these grains contain sulfide and other non-oxide phases too.

Among these analyzed opaque minerals, *i.e.* taenite, magnetite, troilite and pentlandite, taenite is ferromagnetic and magnetite is ferrimagnetic, whereas stoichiometric troilite (FeS) is antiferromagnetic. The basic magnetic properties of pentlandite, $(Fe, Ni)_9S_8$, have not yet been experimentally well known, but theoretically this mineral will be antiferromagnetic. It does not seem, however, that all the so-called troilite phases in the Allende have the chemical composition near the stoichiometric FeS, being antiferromagnetic in their magnetic property, but some of them could be ferrimagnetic pyrrhotite. In order to examine a possibility mentioned above, fine grains (less than 300 μm in mean diameter) made by crushing a bulk sample of the Allende are magnetically separated into magnetic and non-magnetic groups. Chemical compositions of typical magnetic and non-magnetic fine grains, measured by EPMA, are summarized in Table 3, where the major parts of the magnetic fine grains are either troilite or taenite, whereas the major parts of all the non-magnetic fine grains are pentlandites. Although a considerable defect of total mass is seen for some fine grains such as (1) and (4), probably owing to co-existence of silicates in these grains, an approximate interpretation of magnetic properties of the magnetic grains may be derived from the chemical data given by Table 3. For both 2 taenite grains (3) and (4), Ni/(Fe+Ni) is 69 wt %, while $x=0.09$ for troilite grain (1) and $x=0.14$ for troilite grain (2) in terms of FeS_{1+x}. Since FeS_{1+x} is ferrimagnetic for $1/10 \leqq x \leqq 1/7$ (*e.g.* NAGATA, 1961), it is highly probable that troilite grains (1) and (2) are ferrimagnetic pyrrhotites.

Table 3. Chemical composition of magnetic and non-magnetic fine grains (wt %).

	Magnetic				Non-magnetic				
	(1) Tr	(2) Tr	(3) Fe-Ni	(4) Fe-Ni	(5) Pe	(6) Pe	(7) Pe	(8) Pe	(9) Pe
Fe	58.39	60.49	29.65	28.31	41.41	45.71	43.98	45.11	49.92
Ni	0.31	1.30	66.57	62.57	21.89	20.85	19.85	18.51	22.30
Co	0.12	0.02	1.64	1.62	1.21	1.15	1.10	1.10	1.13
S	34.68	37.52	0.01	0.03	33.07	33.84	32.31	32.31	33.07
Total	93.50	99.33	97.87	92.53	97.58	101.55	97.24	97.03	102.42

4. Basic Magnetic Properties of the Allende

The saturation magnetization (I_s), saturated isothermal remanent magnetization (I_R), coercive force (H_c) and remanence coercive force (H_{RC}) of 2 bulk samples of the Allende measured at 16°C and -269°C are summarized in Table 4, where these magnetic parameters of other bulk samples of the Allende at room temperature reported in previous works (BRECHER and ARRHENIUS, 1974; NAGATA, 1979a) also are given for reference.

The I_s-values range from about 0.5 emu/g to about 1.3 emu/g at room temperature as shown in Table 4, where masses of individual examined samples are 10–100 mg.

It is certain therefore that the distributions of ferromagnetic and ferrimagnetic constituents are not uniform in mass scale of 10–100 mg in the Allende, but ratio of their largest content to their smallest one amounts to about three. Similarly, the I_R-values range from about 0.05 emu/g to about 0.26 emu/g at room temperature, ratio I_R/I_s ranging from 0.08 to 0.20. The observed dispersion of I_R/I_s-values may suggest that not only the content of ferromagnetic/ferrimagnetic constituent but its composition also is considerably heterogeneous in mass scale of 10–100 mg in the Allende. A significant characteristic of the magnetic properties of the bulk samples of the Allende chondrite is that the magnetic coercive force (H_c) is considerably large, being 140–180 Oe at room temperature, throughout all examined samples listed in the table. The high magnetic

Table 4. Basic magnetic parameters of bulk samples of the Allende.

Temperature	Sample A		Sample B		Previous data	
					Brecher and Arrhenius (1974)	Nagata (1979a)
	16°C	−269°C	16°C	−269°C	Room temperature	
I_s (emu/g)	1.31	1.55	0.80	0.76	0.48–0.73	0.61
I_R (emu/g)	0.26	0.48	0.13	0.18	0.06	0.048
H_c (Oe)	175	270	180	300	138±3	140
H_{RC} (Oe)	530	930	590	1430	—	800
Θ_c (°C)	610		615		—	576 620
Sample mass (mg)	106		85		(8–12)	21

coercivity of the Allende indicates a high stability of its remanent magnetization which is the main subject of the present study. Such a large value of H_c, 150–200 Oe, often takes place in terrestrial basalts (*e.g.* NAGATA, 1961). In the case of terrestrial basalts, the observed large H_c is attributed to the presence of very fine grains (less than 10 μm in average diameter) of magnetite (*e.g.* NAGATA, 1961). It would be possible to presume that the observed large value of H_c of the Allende also is attributable, at least partially, to such fine grains of magnetite. It is further possible that an additional small amount of pyrrhotite components in the iron-sulfide grains enlarges the apparent value of H_c, because the magnetic anisotropy energy of a hexagonal crystal of pyrrhotite is very large, being 3×10^7 emu/cm^3 in the order of magnitude at room temperature for a stoichiometric pyrrhotite, Fe_7S_8 (BIN and PAUTHENET, 1963).

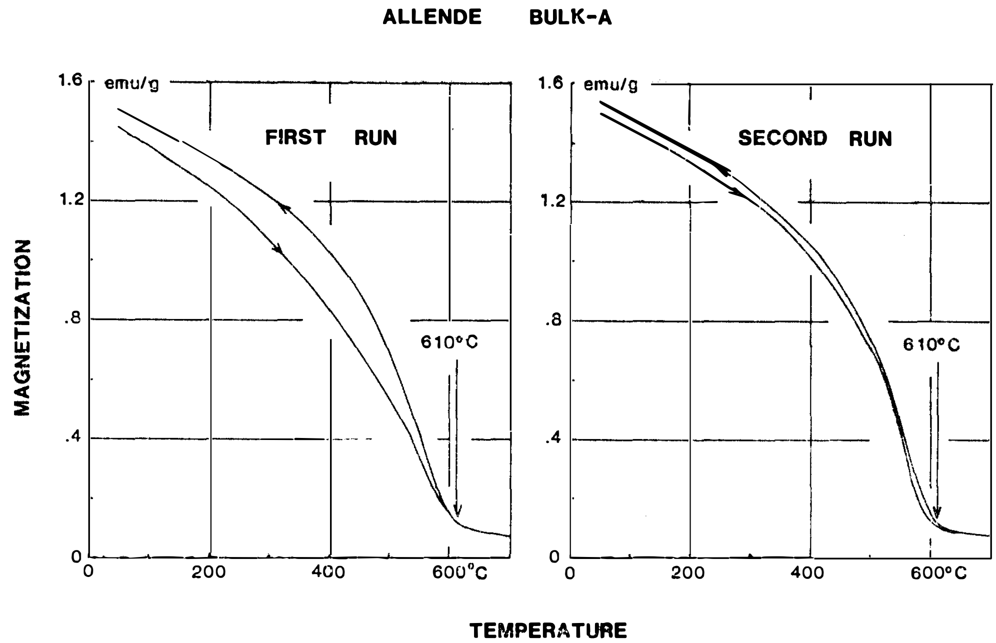

Fig. 2. Thermomagnetic curves of a bulk specimen (A) of the Allende, first-run and second-run curves (magnetic field=10 kOe).

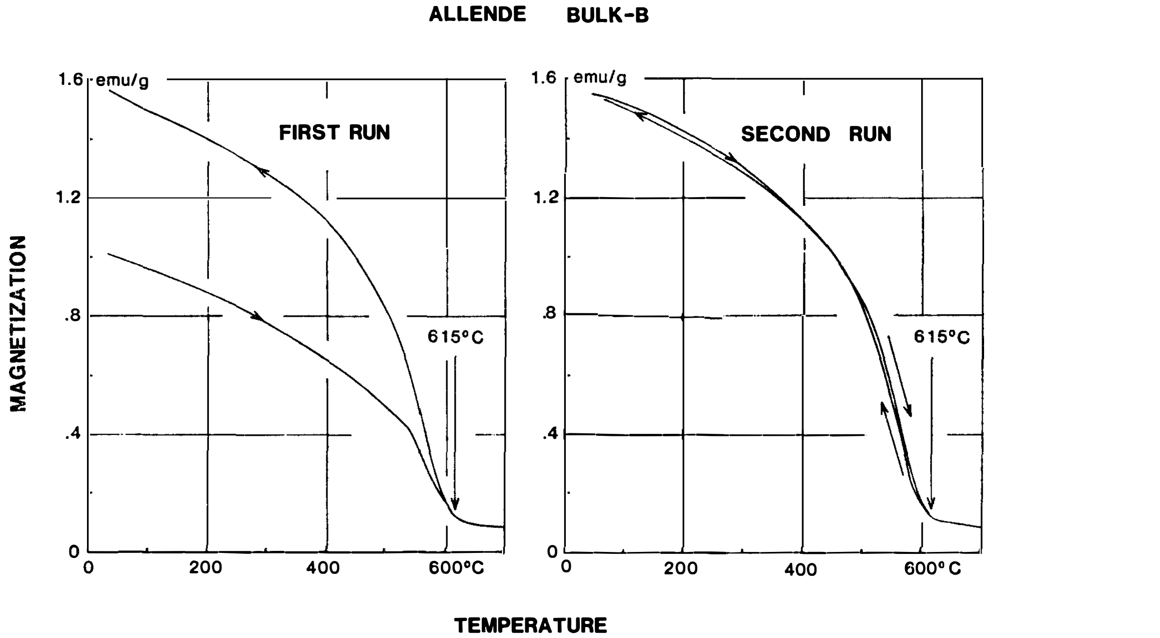

Fig. 3. Thermomagnetic curves of a bulk specimen (B) of the Allende, first-run and second-run curves (magnetic field = 10 kOe).

The thermomagnetic curves of two bulk samples of the Allende, observed in an external magnetic field of 10 kOe, are shown in Figs. 2 and 3. As summarized in Table 4, the major Curie point is 610–615°C, and no definite magnetic transition can be detected on the thermomagnetic curves around 320°C, which corresponds to Curie point of pyrrhotite. The content of phrrhotite is therefore to be very small. The observed Curie point at 610–615°C is very likely to represent taenite of 65–73 wt % Ni in its Fe-Ni composition (CRANGLE and HALLAM, 1963). The chemical composition of taenite thus estimated from the Curie point value is in good agreement with that of taenite grains observed by EPMA in the present study as well as by HAGGERTY and MCMAHON (1979).

Although fine grains of magnetite are present in both chondrules and matrix of the Allende, Curie point of magnetite (lower than 580°C) cannot be distinctly detected on the observed thermomagnetic curves. This result suggests that the content of magnetite is relatively small in comparison with that of metallic taenite in the Allende, or the thermomagnetic curve of magnetite superimposes that of taenite phases whose Curie points spread from 615°C down to 580°C or lower temperature dependent on Ni-content from 69 wt % down to 59 wt % or less.

5. Natural Remanent Magnetization of the Allende

It has been reported that the natural remanent magnetization (NRM) of the Allende is extremely stable in the AF-demagnetization test; namely, ratio of the residual intensity of NRM after AF-demagnetizing to 500 Oe peak ($I_n(500)$) to the initial intensity before the AF-demagnetization ($I_n(0)$) is given by $I_n(500)/I_n(0) = 0.87$ (BANERJEE and HARGRAVES, 1972), 0.63 (BRECHER and ARRHENIUS, 1974) and 0.83 (NAGATA, 1979a).

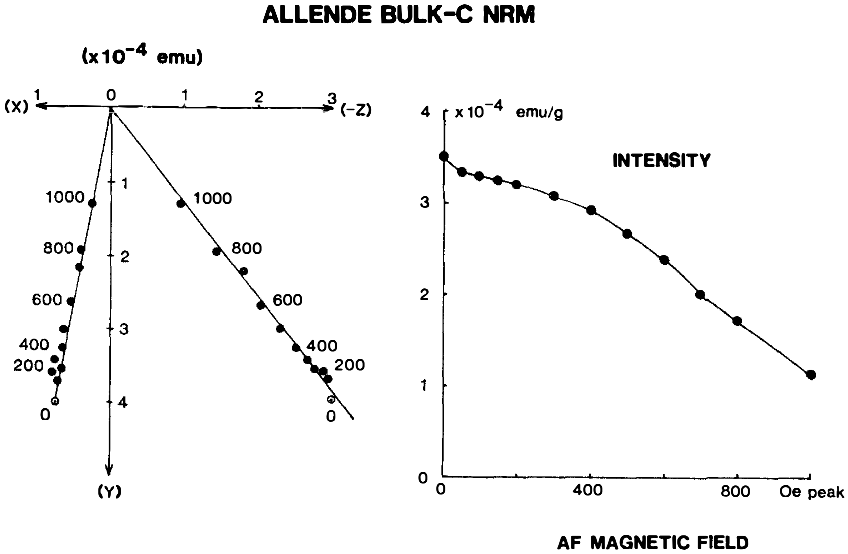

Fig. 4. AF-demagnetization curves of NRM of a bulk specimen (C) of the Allende. (Numeral figures for plots in the left diagram are Af-demagnetizing fields in unit of Oe peak.)

An example of the AF-demagnetization test for NRM of an Allende bulk sample is illustrated in Fig. 4. In this example also, $I_n(500)/I_n(0)=0.76$, and the directions of NRM components which are AF-demagnetized by alternating magnetic field up to 1000 Oe peak are approximately uniform, as illustrated on the left-side diagram of Fig. 4.

For the purpose of examining uniformity and stability of NRM of the bulk specimen of Allende, a plate-form specimen of about 2 mm in thickness is chipped into 15 pieces of 100–300 mg in weight, where the orientations of individual chips are determined with respect to the coordinates of the original plate-form specimen. In Table 5 the specific intensity of NRM, $I_n(0)$, and the declination (D_0) and inclination (I_0) of NRM direction with respect to the coordinates are given for the 15 chips together with their weights. The intensity and direction of the initial NRM of the 15 individual pieces are reasonably well uniform as indicated by $\overline{I_n(0)}=(2.29\pm0.15)\times10^{-4}$ emu/g and $\alpha_{95}=5.2°$. Then, a low temperature cleaning of NRM (*e.g.* OZIMA and NAGATA, 1964) was applied on these chip specimens at the liquid N_2 temperature in order to clean up possible effects of isothermal remanent magnetization (IRM) and/or viscous remanent magnetization (VRM) of the magnetite component in the Allende. Results of the low temperature cleaning of NRM are summarized in the 4th column (liquid N_2 cleaning) of Table 5, where $I_n(L.C.)$ denotes the NRM intensity after the liquid N_2 temperature cleaning, and ΔD and ΔI give deviations of the declination and inclination of NRM after the cleaning treatment from D_0 and I_0 respectively. By the low temperature cleaning treatment the uniformity of Allende NRM is a little changed, as indicated by $\overline{I_n(L.C.)}=(2.23\pm0.09)\times10^{-4}$ emu/g and $\alpha_{95}=7.5°$. In Fig. 5, the distribution of the direction of NRMs of the 15 chip specimens are illustrated.

The intensity ($I_n(100)$) and deviations of declination ($\Delta'D$) and inclination ($\Delta'I$) from D_0 and I_n respectively of the residual NRM after an AF-demagnetization treatment up to 100 Oe peak of these 15 chip specimens which were previously cleaned at

Table 5. Low temperature cleaning and AF-demagnetization of NRM of bulk specimens.

Specimen	Weight	NRM			Liquid N_2 cleaning			AF-demag. ($\tilde{H}=100$ Oe peak)		
		$I_n(0)$ ($\times 10^{-4}$emu/g)	D_0 (degree)	I_0	$I_n(L.C.)$ ($\times 10^{-4}$emu/g)	ΔD (degree)	ΔI	$I_n(100)$ ($\times 10^{-4}$emu/g)	$\Delta' D$ (degree)	$\Delta' I$
(A–1)										
(1)	345	2.02	−28	3	2.17	+9	+19	2.03	+7	+22
(2)	207	2.20	−17	24	2.41	−12	−8	2.44	+7	+15
(3)	189	1.84	−18	25	2.14	+1	−5	2.09	+5	−1
(4)	184	2.33	−22	25	2.23	+5	−6	2.11	+2	+1
(5)	194	2.27	−27	35	2.15	+7	−19	2.00	+12	−12
(6)	109	2.62	−35	48	2.47	+27	−38	2.19	+30	−21
(7)	157	2.42	−17	26	2.38	+3	−16	2.29	+5	+2
(8)	119	2.25	−19	31	2.19	+21	−4	2.18	+12	−3
(9)	115	2.23	−28	37	2.15	+9	+24	1.87	+6	−9
(10)	144	2.78	−23	22	2.18	−17	+3	2.07	+7	+6
(11)	187	2.32	−16	22	2.19	−9	+3	2.05	+1	−3
(12)	197	2.32	−18	28	2.23	−7	−10	2.04	+3	+1
(13)	185	2.40	−29	35	2.31	+2	−4	2.06	+17	−9
(14)	114	2.27	−22	15	2.20	+14	−7	2.11	+6	+1
(15)	103	2.07	−19	34	1.97	+11	−7	1.78	+6	−7
Average		2.29	−22.5	27.3	2.23	+4.3	−5.0	2.09	+8.4	−1.1

$I_n(0)$: Initial intensity of NRM.
D_0: Initial declination of NRM.
I_0: Initial inclination of NRM.
$I_n(L.C.)$: Intensity of NRM after liquid N_2 temperature cleaning.
ΔD: Deviation angle of NRM declination after liquid N_2 temperature cleaning from D_0.
ΔI: Deviation angle of NRM inclination after liquid N_2 temperature cleaning from I_0.
$I_n(100)$: Intensity of NRM after AF-demagnetizing $I_n(L.C.)$ to 100 Oe peak.
$\Delta' D$: Deviation of declination of $I_n(100)$ from D_0.
$\Delta' I$: Deviation of inclination of $I_n(100)$ from I_0.

the low temperature are summarized in the last column (AF-demag.) of Table 5, where $\overline{I_n(100)}=(2.09\pm 0.11)\times 10^{-4}$ emu/g and $\alpha_{95}=3.4°$. As shown in the table, effects of the AF-demagnetization are small, $\overline{I_n(100)/I_n(L.C.)}$ and $\overline{I_n(100)/I_n(0)}$ being 0.94 and 0.91 respectively. The top diagram of Fig. 6 shows a histogram of $I_n(100)/I_n(0)$ of 15 individual chip specimens. It may be generally concluded, therefore, that NRMs of bulk samples of the Allende are uniform and very stable in the AF-demagnetization test, as represented by Fig. 4.

Seventeen chondrules were picked up from 2 bulk specimens of the Allende and their NRM were examined. The weight, NRM of individual chondrules, specific intensity of NRM ($I_n(0)$), ratio of residual NRM intensity after AF-demagnetizing up to 100 Oe peak ($I_n(100)$) to $I_n(0)$, and an angle between the direction of initial NRM and that of residual NRM after the 100 Oe peak AF-demagnetization (Δ 100) are summarized in Table 6. Comparing Table 6 with Table 5, it can be noted that the $I_n(0)$ values of chondrules spread over a wide range from about 1×10^{-5} emu/g to about 3×10^{-3} emu/g and NRMs of a number of chondrules are unstable in the AF-demagnetization only up to 100 Oe peak as suggested by $I_n(100)/I_n(0)<0.8$ or $\Delta 100>30°$. Further,

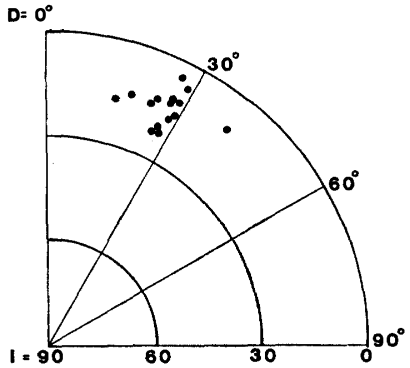

Fig. 5. *Distribution of the directions of NRM of 15 chips of the bulk Allende after the low temperature cleaning at liquid N_2 temperature.*

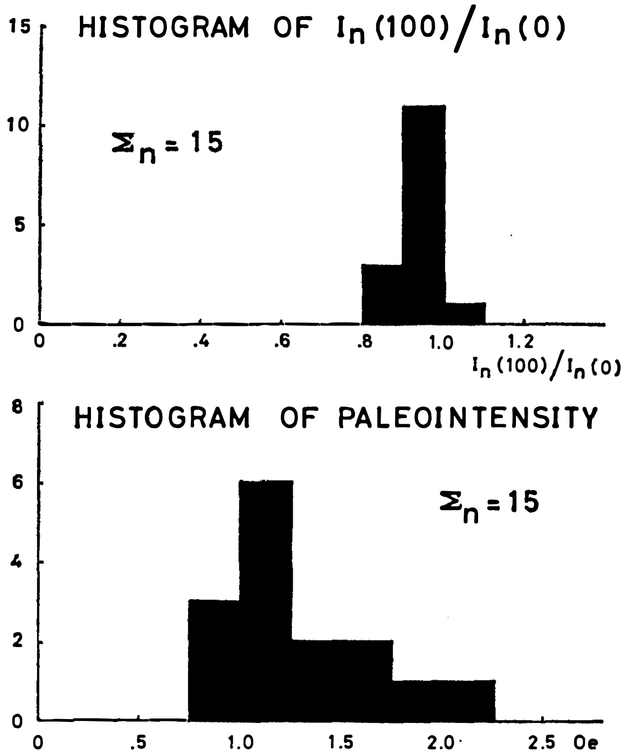

Fig. 6. *(Top) Histogram of ratios of residual NRM intensity (I_n (100) after AF-demagnetizing to 100 Oe peak to initial NRM intensity (I_n (0)) for 15 chips of the Allende bulk rock. (Bottom) Histogram of paleointensities for 15 chips of the Allende bulk rock.*

some chondrules possess a very weak NRM, $I_n(0)$ being smaller than 1×10^{-4} emu/g, in comparison with NRM of the bulk specimen, which is $(2.0\text{–}2.8)\times10^{-4}$ emu/g (Table 5). In the present study in addition, quantitative magnetic measurements of NRM of individual chondrules whose NRM moment is smaller than 1×10^{-6} emu/sample are practically unreliable.

If those chondrules of $M_n(0)\lesssim1\times10^{-6}$ emu/sample or $I_n(100)/I_n(0)<0.8$ or $\Delta100\gtrsim 30°$ are regarded as magnetically unreliable and/or unstable chondrules so that they are to be rejected form Table 6, (A-1-2) chondrule only can remain as a reasonably reliable sample having a stable NRM, all other 16 chondrules being rejected. An AF-demagnetization curve of (A-1-2) chondrule up to $\tilde{H}=100$ Oe peak is shown in the left diagram of Fig. 7, where the AF-demagnetization curves of (A-2-2) and (A-2-3) chondrules also are illustrated for comparison. Wasilewski and Saralker (1981) also examined the stability of NRM of 20 chondrules chosen at randum from the Allende. Among the 20 chondrules, 6 have the stable NRM of $I_n(100)/I_n(0)\simeq1$ and $\Delta100<10°$, whereas NRMs of the other 14 chondrules are unstable.

In contrast to the chondrules, NRM of the matrix of the Allende is generally stable, as shown in Table 7, where weight, $M_n(0)$, $I_n(0)$, $I_n(100)/I_n(0)$ and $\Delta100$ of 3 specimens of matrix are summarized. The right-side diagram of Fig. 7 shows the AF-de-

Table 6. AF-demagnetization of chondrules.

Chondrules	Weight (mg)	$M_n(0)$ (emu)	$I_n(0)$ (emu/g)	$I_n(100)/I_n(0)$	$\Delta 100$ (degree)
A-1-1	13	1.03×10^{-6}	0.79×10^{-4}	0.98	23
A-1-2	23	5.87 〃	2.55 〃	0.99	2
A-1-3	6.0	0.98 〃	1.63 〃	0.60	20
A-1-4	18	0.27 〃	0.16 〃	2.02	10
A-1-5	5.6	0.36 〃	0.63 〃	0.39	90
A-1-6	4.7	0.36 〃	0.76 〃	1.00	0
A-2-1	18	1.69×10^{-5}	9.40 〃	0.06	31
A-2-2	31	6.26 〃	20.10 〃	0.21	19
A-2-3	8.4	2.35 〃	29.33 〃	0.38	3
A-2-4	8.4	2.12×10^{-6}	2.65 〃	0.44	40
A-2-5	15	1.88 〃	1.25 〃	0.55	30
A-2-6	64	0.77 〃	0.12 〃	0.95	23
A-2-7	9.0	0.58 〃	0.65 〃	1.35	96
A-2-8	16	0.24 〃	0.15 〃	0.92	57
A-2-9	4.5	0.31 〃	0.63 〃	0.71	91
A-2-10	20	0.38 〃	0.19 〃	0.96	19
A-2-11	26	0.82 〃	0.31 〃	0.72	24

$M_n(0)$: Magnetic moment of NRM per individual chondrule.
$I_n(0)$: Specific intensity of initial NRM.
$I_n(100)$: Residual NRM intensity after AF-demagnetizing to 100 Oe peak.
$\Delta 100$: Angle between the direction of initial NRM and that of residual NRM after 100 Oe peak AF-demagnetization.

Table 7. AF-demagnetization of matrix.

Matrix	Weight (mg)	$M_n(0)$ (emu)	$I_n(0)$ (emu/g)	$I_n(100)/I_n(0)$	$\Delta 100$ (degree)
(1)	29.3	7.17×10^{-6}	2.45×10^{-4}	1.02	7
(2)	22.2	7.04 〃	3.18 〃	0.94	11
(3)	15.3	4.84 〃	3.17 〃	0.97	4

magnetization curves of NRM of the 3 matrix specimens. It is demonstrated in Fig. 7 that the AF-demagnetization characteristics of NRM of the matrices are almost exactly same as those of NRM of magnetically stable chondrule (A-1-2) but are markedly different from those of magnetically unstable chondrules (A-2-2) and (A-2-3). Another point worthwhile to be noted in Table 7 and in Fig. 7 will be the fact that the initial intensity of NRM, $I_n(0)$, of matrix is in a range of $(2.5\text{–}3.2)\times10^{-4}$ emu/g which is roughly same in the order of magnitude as $I_n(0)$ of the stable chondrule (A-1-2) as well as that of the bulk samples of the Allende chondrite illustrated in Fig. 4 and summarized in Table 5. (The $I_n(0)$ values of 17 chondrules in Table 6 may be divided into 3 groups; namely, 4 chondrules of $1.0\times10^{-4}<I_n(0)<4.0\times10^{-4}$ emu/g, 10 chondrules of $I_n(0)<1.0\times10^{-4}$ emu/g and 3 chondrules of $I_n(0)>5\times10^{-4}$ emu/g.) It seems very likely thus that the uniform and stable NRM of bulk specimen of the Allende chondrite is mostly due to the stable NRM of the matrix parts.

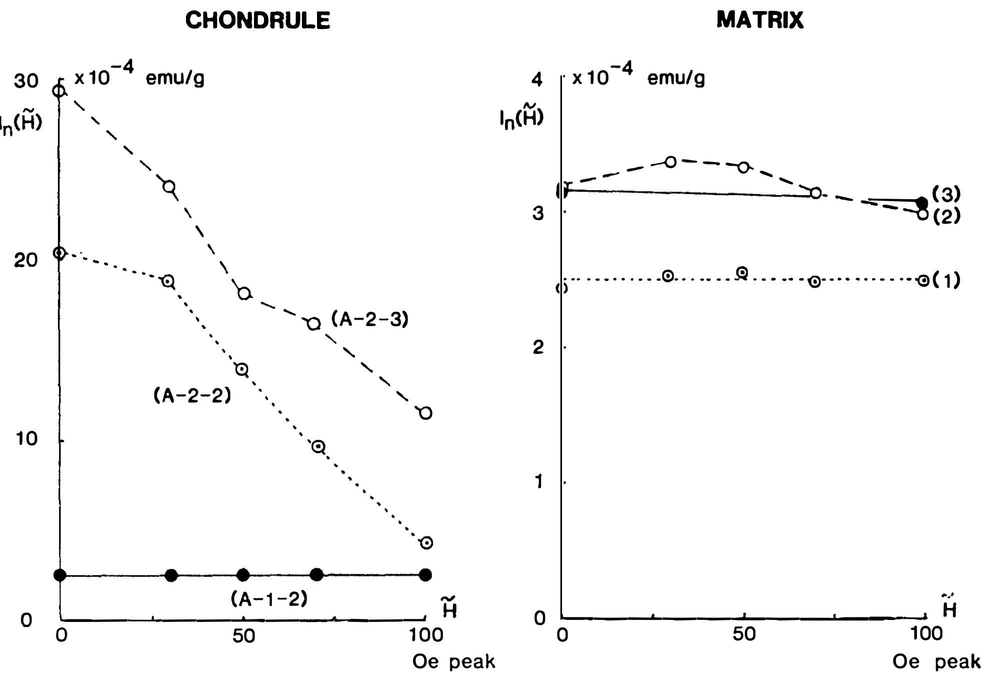

Fig. 7. AF-demagnetization curves to 100 Oe peak of NRM for 3 Allende chondrules and 3 pieces of Allende matrix.

6. Thermal Demagnetization Characteristics of NRM

The thermal demagnetization test was applied first on NRM of the bulk specimens of the Allende chondrite. In the heating-cooling cycle experiments in the thermal demagnetization, the Taylor's method was adopted for holding an examined sample. Figure 8 illustrates an example of the thermal demagnetization curves for the direction (top) and the intensity (bottom) of NRM of a bulk sample, A-2 (weight = 772 mg). As shown in the projections of residual NRM on the X-Y and Y-Z planes during the course of thermal demagnetization, NRM of the Allende bulk specimen is of a single unidirection phase, and it is thermally demagnetized almost completely at 310–330°C (top and bottom diagrams).

Other 3 examples of the thermal demagnetization of NRM of the bulk specimens are shown in Fig. 9, where weights of Allende-G, -H and -I samples are 1123, 427 and 293 mg respectively. All these 3 bulk specimens also indicate that their NRM comprises only a single unidirectional phase which can be thermally demagnetized almost completely at about 320°C. Since both matrix and chondrules of the Allende contain pyrrhotite, Curie point of which is 320°C, it will be most likely that the pyrrhotite phase possesses the observed NRM.

For the purpose of confirming the thermal demagnetization characteristics of the bulk NRM, 15 bulk specimens, which have been AF-demagnetized to 100 Oe peak (Table 5), are thermally demagnetized by heating to 380°C. The residual remanent magnetization after the thermal demagnetization is summarized in Table 8, where ratio of the residual remanent magnetization intensity, $I_n(380°C)$, to $I_n(100)$ also is given for each specimen. As $I_n(380°C)/I_n(100) < 0.04$ throughout all 15 bulk specimens, it may

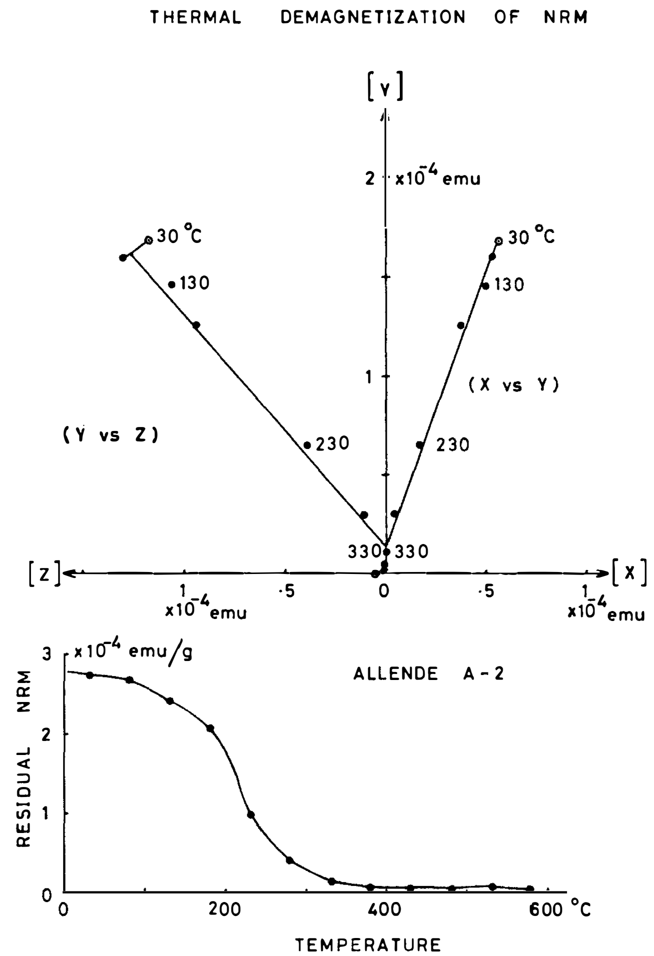

Fig. 8. Thermal demagnetization curves of NRM of Allende bulk specimen (A-2).
(Top) Projection of residual NRM vectors on (X-Y) and (Y-Z) planes.
(Bottom) Thermal demagnetization curve of NRM intensity.

be concluded that the bulk NRM of the Allende is thermally demagnetized almost completely by heating to 380°C.

Then, the same thermal demagnetization test is applied on 3 matrix specimens given in Table 7 and illustrated in Fig. 7 and on 3 chondrule specimens illustrated in Fig. 7. As shown in the left-side diagram of Fig. 10, almost all portions of NRMs of the three matrix specimens are thermally demagnetized by heating to about 320°C. The direction of residual NRM of these matrix specimens during the thermal demagnetization process is kept approximately constant as in the case of bulk specimens. The right-side diagram of Fig. 10 illustrates a thermal demagnetization curve of chondrule possessing stable NRM, (A-1-2). The NRM of this chondrule of stable NRM also is thermally demagnetized almost completely at about 320°C. For comparison, the residual NRMs after AF-demagnetizing to 100 Oe peak of 2 chondrules (A-2-2 and A-2-3), whose NRMs are not stable in the AF-demagnetization, are thermally demagnetized. As shown in Fig. 11, it appears that the thermal demagnetization curves of

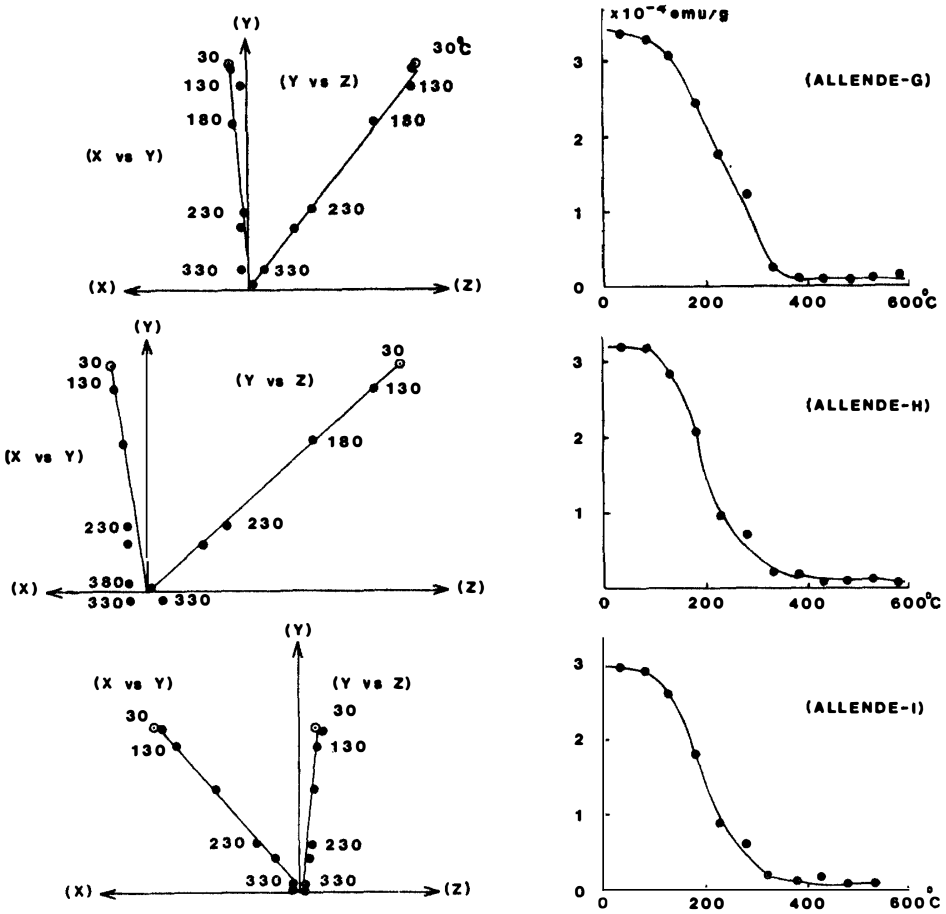

Fig. 9. Thermal demagnetization curves of NRM of 3 Allende bulk specimens (G, H and I).
(Left) Projections of residual NRM vectors on (X-Y) and (Y-Z) planes.
(Right) Thermal demagnetization curves of NRM intensity.

the residual NRMs of the two chondrules consist of, at least, two steps, *i.e.* a component which can be thermally demagnetized at about 300°C and the other component which can be thermally demagnetized at about 600°C. Since, as shown in Fig. 7, the major parts of NRM of these two chondrules have already been AF-demagnetized by $\tilde{H}=100$ Oe peak magnetic field before the thermal demagnetization experiment, the thermomagnetic characteristics of the whole magnetic phases concerning NRM in the initial state of these chondrules are not represented by Fig. 11. If we assume, however, that a ferro- or ferri-magnetic phase possessing NRM which is thermally demagnetized almost completely at about 320°C (which is very likely to be identified as pyrrhotite) is included in these chondrules also, then the NRM component possessed by the apparent pyrrhotite phase should remain approximately invariable even after the AF-demagnetization up to 100 Oe peak. The NRM component which is thermally demagnetized at about 300°C in Fig. 11 may probably be identified as NRM of this apparent pyrrhotite. The other NRM component may be possessed by either Ni-rich taenite or magnetite or both, because its magnetic transition temperature is about 600°C. If we assume that the acquisition of original NRM of these chondrules is shared

Table 8. Thermal demagnetization of NRM and acquistion of PTRM of bulk specimens.

Specimen	$I_n(100)$ ($\times 10^{-4}$emu/g)	I_n (380°C) ($\times 10^{-4}$emu/g)	$\frac{I_n\ (380°\text{C})}{I_n(100)}$	PTRM $H=0.44$ Oe $T_0=330$°C ($\times 10^{-4}$emu/g)	F_p (Oe)
(1)	2.03	0.056	0.028	0.834	1.07
(2)	2.44	0.044	0.018	0.670	1.60
(3)	2.09	0.063	0.030	0.743	1.23
(4)	2.11	0.074	0.035	0.887	1.05
(5)	2.00	0.073	0.036	1.017	0.87
(6)	2.19	0.067	0.031	0.520	1.85
(7)	2.29	0.043	0.019	0.597	1.69
(8)	2.18	0.059	0.027	0.472	2.04
(9)	1.87	0.009	0.005	0.728	1.13
(10)	2.07	0.042	0.020	0.719	1.27
(11)	2.05	0.016	0.008	1.041	0.87
(12)	2.04	0.019	0.009	0.771	1.16
(13)	2.06	0.054	0.026	0.739	1.23
(14)	2.11	0.085	0.040	0.676	1.37
(15)	1.78	0.078	0.044	0.995	0.79

$I_n(100)$: NRM intensity after AF-demagnetizing to 100 Oe peak.
I_n (380°C): Residual remanent magnetization intensity after thermally demagnetizing to 380°C.
PTRM: $H=0.44$ Oe, $T_0=330$°C: Partial thermoremanent magnetization acquired by cooling from 330°C to 20°C in a magnetic field of 0.44Oe.
F_p: Paleointensity.

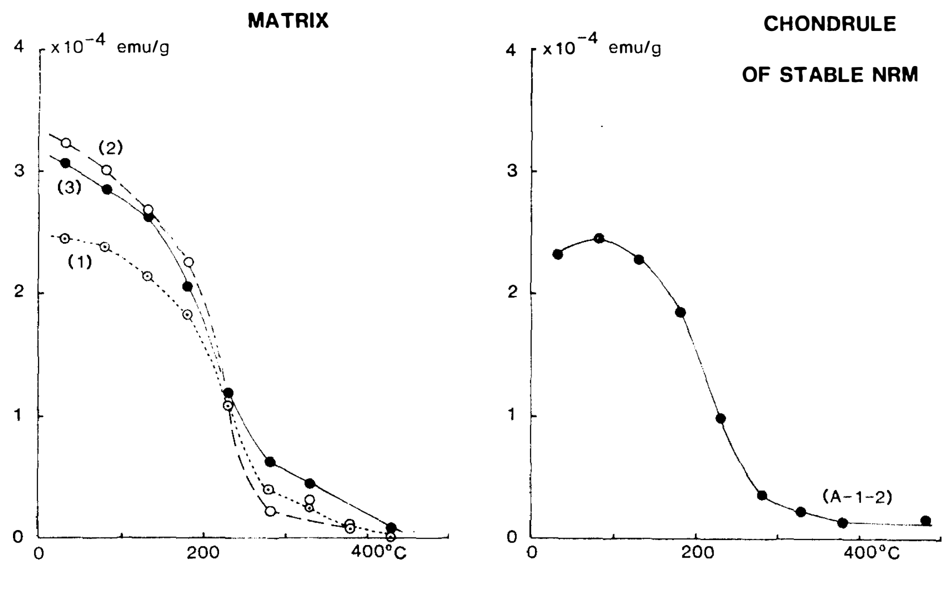

Fig. 10. Thermal demagnetization curves of NRM intensity for 3 pieces of Allende matrix (left) and Allende chondrule which has stable NRM (right).

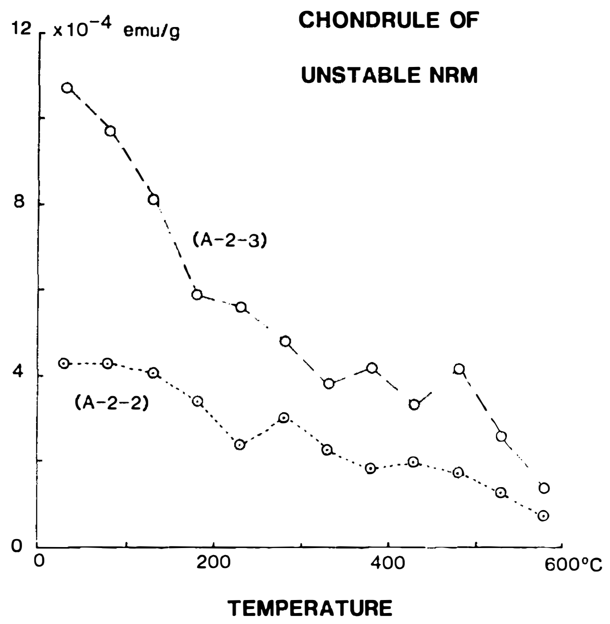

Fig. 11. Thermal demagnetization curves of NRM intensity for 2 Allende chondrules which have unstable NRM.

mostly by the apparent pyrrhotite phase and the Ni-rich taenite/magnetite phase, the larger parts of their NRM which are AF-demagnetized by 100 Oe peak field are attributable to remanent magnetization of the Ni-rich taenite/magnetite phase, because no other ferro- or ferri-magnetic phase is detected in the Allende and the NRM component of the apparent pyrrhotite is almost constant within the AF-demagnetization field range. In the results of thermal demagnetization experiment of NRM of 2 chondrules, a white inclusion and a piece of matrix of the Allende carried out by SUGIURA *et al.* (1979), NRM of the matrix is thermally demagnetized almost completely at 320°C, whereas the thermomagnetic curves of the two chondrules have almost the same characteristics as those shown in Fig. 11. These results are in good agreement with the conclusion of the present study.

An important point of the results of magnetic studies of the Allende by SUGIURA *et al.* (1970) may be a finding that the direction of NRM in individual chondrules is widely scattered but loosely clustered in a hemisphere. From the observed thermal demagnetization characteristics of NRM, on the other hand, it seems most likely that NRM of the bulk specimens of the Allende is substantially attributable to NRM of its matrix as far as test bulk specimens have sufficiently large size compared with the size of chondrules which have NRM of semi-random orientations. When the AF-demagnetization cleaning technique up to 100 Oe peak is applied on original NRM, in particular, the cleaned NRM of a bulk specimen can be almost attributed to NRM of matrix.

If we consider that the uniform and stable component of NRM of matrix which is thermally demagnetized at 320°C is possessed by the apparent pyrrhotite phase, a puzzling point will be that no magnetic transition of this phase can be detected on the thermomagnetic curves shown in Figs. 2 and 3. WASILEWSKI and SARALKER (1981), however, found magnetic transition points at 150° and 320°C in addition to the major magnetic transition at 575°C on thermomagnetic curves of some chondrules of the

Allende. As the saturation magnetization intensity (I_s) of stoichiometric pyrrhotite is 23 emu/g, it is much smaller than I_s=120–130 emu/g of taenite of (66–72) wt% Ni and I_s=92 emu/g of magnetite. Even so, the relative content of pyrrhotite in the Allende should be so small that its magnetic transition is not clearly detected on the thermomagnetic curve of a bulk sample of the Allende. As far as NRM of the Allende is concerned, however, it is certain that the majority of its NRM is possessed by the apparent pyrrhotite phase.

A possible experimental simulative demonstration of an acquisition of thermoremanent magnetization of pyrrhotite, on the other hand, is associated with a problem of thermal hysteresis phenomenon of pyrrhotite crystal structure; namely, an ordered arrangement of vacant positions in the ferrimagnetic pyrrhotite crystal structure is destroyed at some elevated temperature (*e.g.* NAGATA, 1961). Figure 12 shows 2 examples of the thermomagnetic curve of natural pyrrhotite measured in a magnetic field of 10 kOe. The chemical compositions of this pyrrhotite sample determined using EMPA is given by 60.122 wt% Fe, 0.710 wt% Ni, 0.070 wt% Co, and 39.541 wr% S on average, or approximately (Fe, Ni, Co) $S_{1.13}$. In the case of specimen (A), the thermomagnetic curves were measured in a temperature range from 30° to 660°C. The initial heating thermomagnetic curve may represent the typical thermomagnetic curve of $FeS_{1.11}$, whereas the cooling thermomagnetic curve from 660°C shows no magnetic transition point of the pyrrhotite phase, suggesting that the ferrimagnetic pyrrhotite structure is destroyed by heating up to 660°C. The second-run thermomagnetic curves of this samples is thermally reversible and practically same as the first-run cooling curve, having a much weaker intensity and Curie point of 535°C. The thermomagnetic curves of specimen (B) were measured in a temperature range from 30° to 480°C. The initial heating thermomagnetic curve in this case also shows the typical magnetic character of $FeS_{1.11}$, but the cooling thermomagnetic curve can represent the thermomagnetic curve of pyrrhotite of chemical composition of $0.12 \leqq x$ in FeS_{1+x}.

Since the order-disorder transformation of vacant positions in the crystal structure, dependent on temperature and minor impurity element, is involved in the ferrimagnetic characteristics of pyrrhotite, it has not yet been clear at the present stage whether the observed conspicuous difference between (A) and (B) is due to a difference in the maximum temperature given in the experiments or to a small difference in their chemical composition. The thermomagnetic curves of another specimen (C) taken from the same natural pyrrhotite, measured in a temperature range from 30° to 590°C, are almost exactly same as those of specimen (A). This additional result might suggest that the order-disorder transformation of ferrimagnetic pyrrhotite takes place at a certain temperature between 440° and 590°C, but this problem will need much more precise examinations in the future.

Since, on the other hand, the anhysteretic remanent magnetization (ARM) is not subjected to any thermal effect at all but still can include the remanent magnetization of magnetically highly coercive component such as pyrrhotite, a thermal demagnetization test of ARM of an Allende bulk specimen was carried out in order to detect a possible presence of pyrrhotite phase in the remanent magnetization. Figure 13 shows the thermal demagnetization curve of ARM of an Allende bulk specimen acquired by $\tilde{H}$=1400 Oe peak in the maximum alternating magnetic field and h=0.44 Oe in the

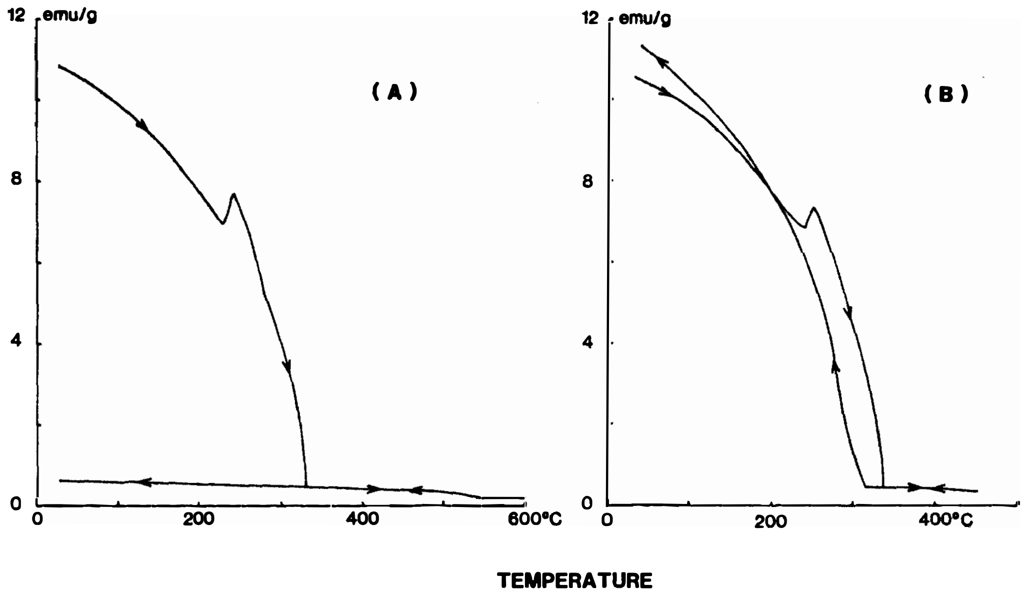

Fig. 12. *Thermomagnetic curves of natural pyrrhotite grains (magnetic field =10 kOe). (A) Heated up to 660°C. (B) Heated up to 480°C.*

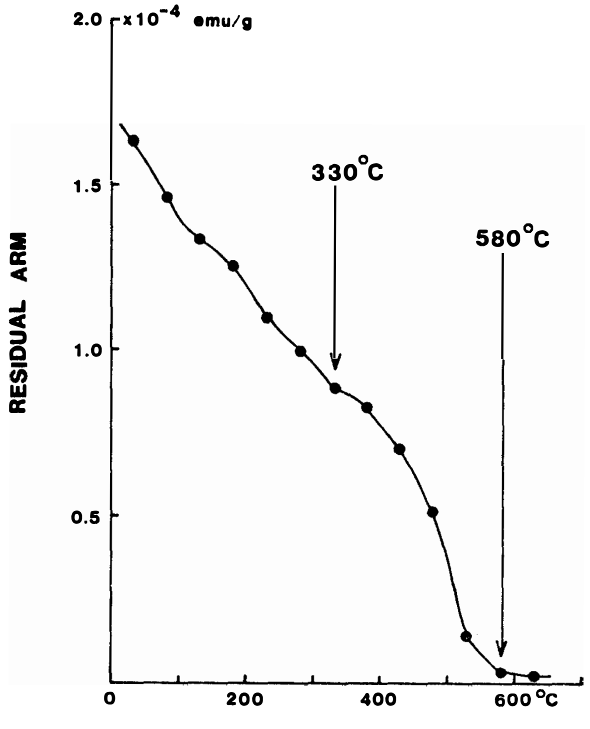

Fig. 13. *Thermal demagnetization curve of ARM intensity of bulk specimen of the Allende (C3). ARM is acquired in $\tilde{H}$ =1400 Oe peak in applied alternating magnetic field and in h=0.44 Oe in coaxially applied steady magnetic field.*

stationary magnetic field. The dependence of thermal demagnetization curve of ARM on temperature in Fig. 13 is considerably different from that of the thermomagnetic curves shown in Figs. 2 and 3; namely, an ARM component having the magnetic transition point at about 330°C can be observed in addition to the taenite/magnetite phase having the magnetic transition point at about 580°C. The ARM component which can be thermally demagnetized at about 330°C occupies about a half of the total ARM and it seems most likely that this component is possessed by the pyrrhotite phase whose Curie point is about 320°C.

7. Paleointensity of the Allende

In the course of experimental process of the thermal demagnetization of NRM, the acquisition experiment of partial thermoremanent magnetization (PTRM) also was carried out using Königisberger-Thellier method with the aid of Taylor technique for each test specimen of the Allende. Figure 14 shows examples of the acquisition curves of PTRM in a magnetic field of 0.44 Oe for 3 bulk specimens, G, H and I, the thermal demagnetization curves of which are shown in Fig. 9. The acquisition rate of PTRM for a temperature range below about 330°C is not large, but it systematically increases with temperature and is almost same among the three examined bulk specimens. As the ordered crystal structure of ferrimagnetic pyrrhotite is not destroyed in a temperature range below 330°C, it seems very likely that a contribution of the pyrrhotite component should be included in PTRM acquired in the temperature range, provided that a certain amount of pyrrhotite is contained in the test bulk specimens. The acquisition rate of PTRM in a temperature range from 330°C to about 500°C also is almost same among the three specimens, but it becomes considerably different from one another

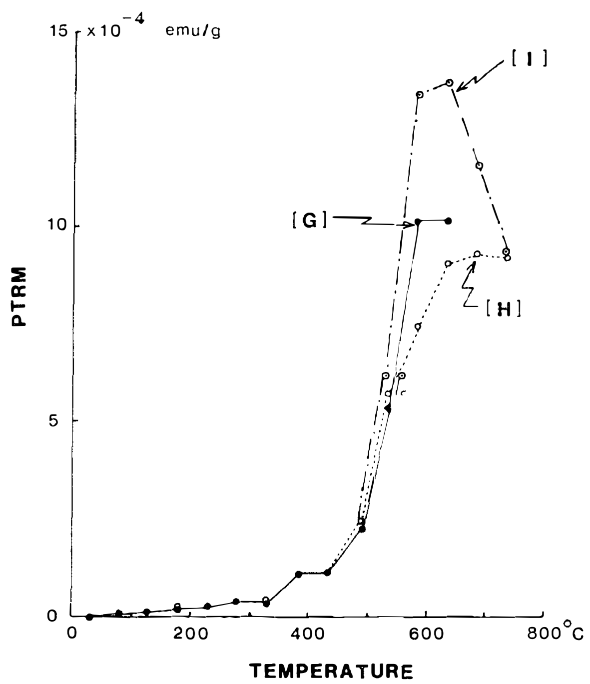

Fig. 14. Acquisition curves of PTRM for 3 pieces (G, H and I) of Allende bulk specimen (magnetic field=0.44 Oe).

in a temperature range above 500°C. In the case of specimen (I), particularly, it can be suggested that some chemical or structural alteration takes place at temperatures above about 600°C.

The PTRM *vs.* temperature curves in Fig. 14 are practically saturated at 580°C for specimens (G) and (I) and at 630°C for specimen (H). It will be obvious in the figure that more than 95% of the total TRM of these bulk specimens are acquired in a cooling process from about 600° to 330°C in a magnetic field regardless whether the pyrrhotite component is destroyed at elevated temperatures above 330°C or not. It will be certain, therefore, that the observed NRM of bulk specimens of the Allende cannot be identified as the total TRM acquired in a cooling process from a temperature higher than 600°C in an approximately constant magnetic field. There would be several different ways for possible mechanism of acquiring the observed NRM of the Allende chondrite. They may be as follows:

(a) There was no or very small magnetic field until the Allende was cooled down to about 320°C, and an ambient magnetic field of F_p was present by some reason during the cooling process below about 320°C.

(b) There was no or very small magnetic field until the Allende chondrite was almost completely formed, but it was reheated up to about 320°C by some reason and then cooled down in the presence of a magnetic field of F_p.

(c) There was no or very small magnetic field until pyrrhotite phase began to be formed, and then a formation of the ferrimagnetic pyrrhotite took place in the presence of F_p so that the chemical remanent magnetization (CRM) or the thermo-chemical remanent magnetization (TCRM) was acquired by the pyrrhotite phase.

Possible cases (a) and (b) are considered on the basis of an assumption that the observed NRM of the Allende may be identified as PTRM of the ferro- and ferri-magnetic phases in the Allende. Figure 15 shows the diagrams of the NRM-lost *vs.* PTRM-gained obtained by Königisberger-Thellier experiment for the three bulk specimens, (G), (H) and (I), the corresponding thermal demagnetization curves and PTRM acquisition curves of which are shown in Figs. 9 and 14 respectively, and Fig. 16 shows the NRM-lost *vs.* PTRM-gained diagram for the largest bulk specimen (A-2), whose thermal demagnetization curve is illustrated in Fig. 8. It may be concluded from all these four examples that a linear relationship holds approximately between the NRM-lost and PTRM-gained in a temperature range from room temperature to about 330°C, but the NRM component remaining at temperatures higher than 330°C is very small, though the bulk specimen is still largely capable to acquire PTRM in the higher temperature range too. The paleointensity (F_p) of the bulk specimen of the Allende can be estimated to be about 3 Oe from Fig. 15 and about 0.9 Oe from Fig. 16.

In order to examine a dispersion of the estimated F_p values, Königisberger-Thellier experiments were carried out on the 15 bulk specimens of the Allende, the thermal demagnetization characteristics of which are summarized in Table 8. The intensities of PTRM of these specimens acquired by cooling from 320°C in a magnetic field of 0.44 Oe are listed in Table 8 together with their F_p values estimated with the Königisberger-Thellier method. As shown in Fig. 6 (bottom), the F_p values of these specimens are distributed in a range between 0.9 and 2.1 Oe. Figure 17 shows the thermal demagnetization curves of PTRM of three typical samples of the bulk specimens (8), (11) and

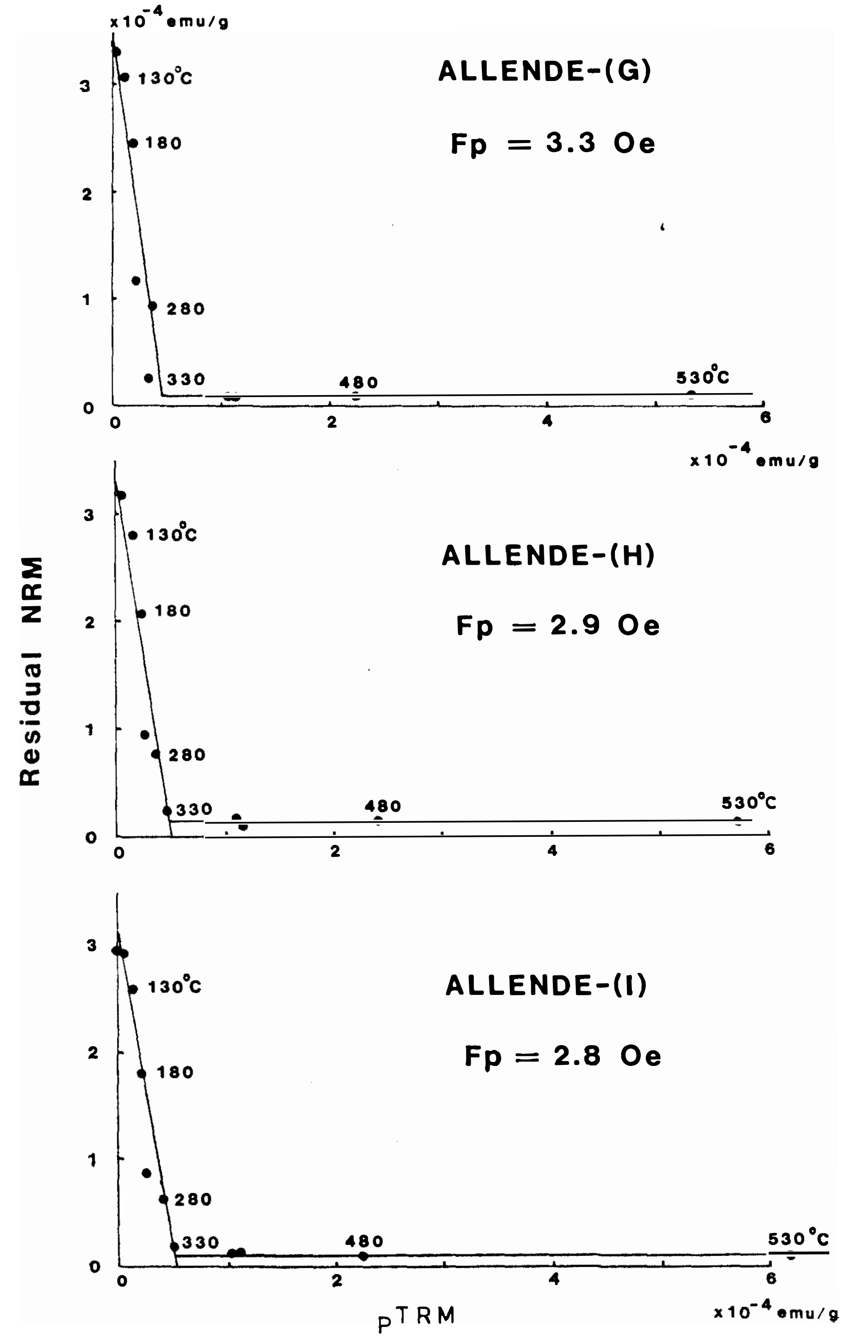

Fig. 15. Königisberger-Thellier plots (NRM-lost vs. PTRM-gained plots) for 3 Allende bulk specimens (G, H and I) (magnetic field for acquisition of PTRM=0.44 Oe).

(12) in Table 8. It appears that general characteristics of these thermal demagnetization curves of PTRM are substantially same as those of NRM of the bulk specimens of the Allende such as shown in Figs. 8 and 9. As far as these experimental data shown in Fig. 6 and Fig. 15 through Fig. 17 are concerned, it may be provisionally concluded that the paleointensity of the Allende chondrite can be estimated to be 1–3 Oe on the assumption of (a) or (b).

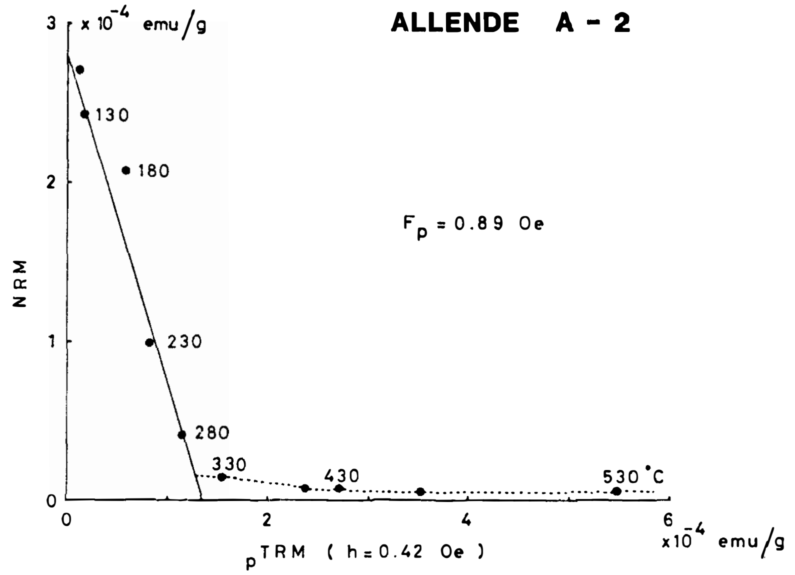

Fig. 16. Königisberger-Thellier plots for Allende bulk specimen (A-2) (magnetic field for acquisition of PTRM=0.42 Oe).

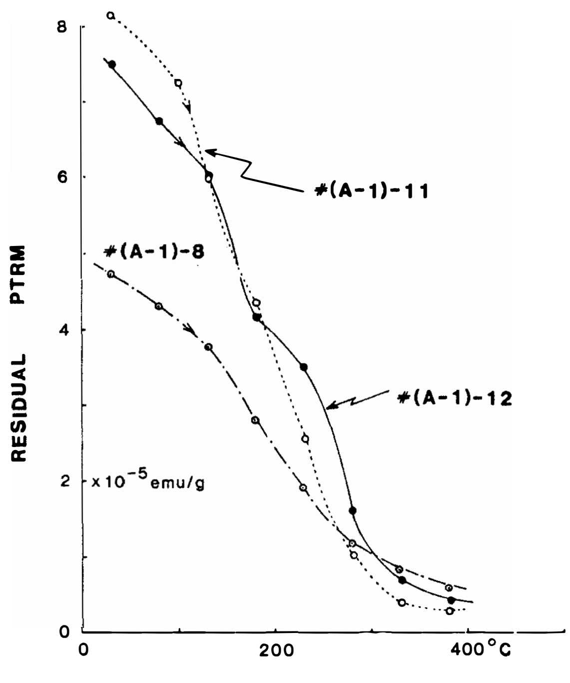

Fig. 17. Thermal demagnetization curves of PTRM which is acquired by cooling from T_{max}=320°C in a magnetic field of H=0.44 Oe for 3 Allende bulk specimens.

If we look at some more detail of the NRM-lost *vs.* PTRM-gained plots in Fig. 15, however, it may be noted that deviations of individual plots from the straight line for an averaged approximation for a temperature range below 330°C have almost the same tendency among the three specimens, (G), (H) and (I). This result may sug-

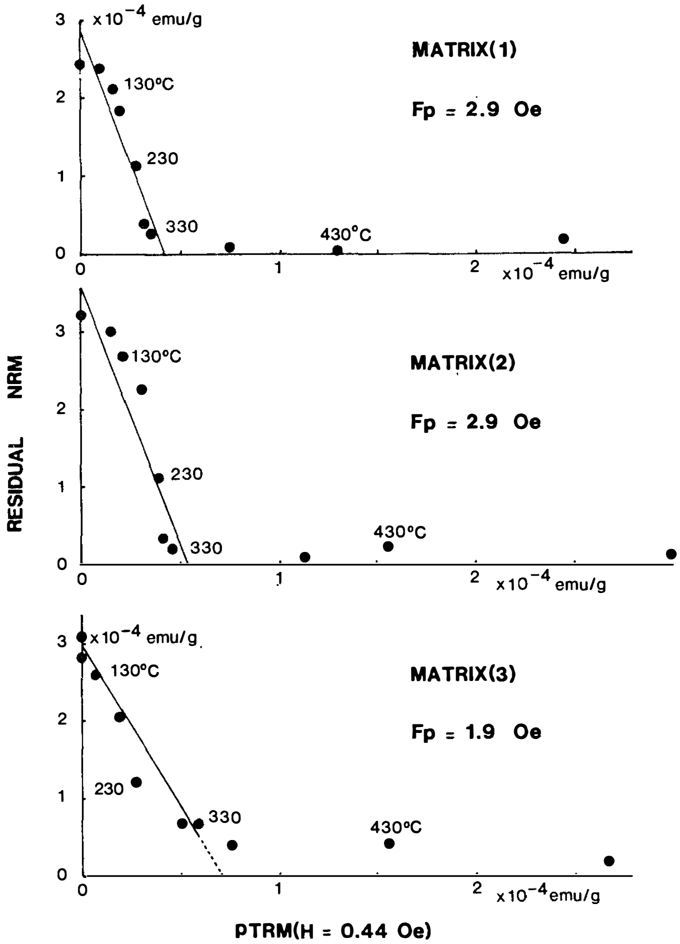

Fig. 18. Königisberger-Thellier plots for 3 Allende matrix specimens (magnetic field for acquisition of PTRM=0.44 Oe).

gest that the deviations are not simply due to experimental errors but probably due to systematic changes in the dependence of both NRM and PTRM on temperature. Although it seems difficult at the present stage to deal with more detail of this problem, thermal change characteristics of the magnetic properties of iron sulfides of FeS $\sim$ Fe_7S_8 in chemical composition will have to be studied more exactly by taking into account possible effects of metallic impurities such as Ni and Co, because it seems most likely that the pyrrhotite phase plays a key role in the stable NRM of the Allende chondrite. For instance, nothing can be discussed at the present stage on a possible mechanism (c) for the acquisition mechanism of the Allende NRM.

Similar experiments to estimate F_p of the separated matrix and chondrule of the Allende with the aid of Königisberger-Thellier method were carried out for comparison. Figure 18 shows the NRM-lost *vs.* PTRM-gained plots for the three matrix specimens, the thermal demagnetization curves of which are shown in Fig. 10. Deviations of individual plots from the expected linear relation between NRM-lost and PTRM-gained in these cases of matrix specimens are larger than those in the cases of bulk specimens (Figs. 15 and 16), largely owing to experimental errors probably caused by the small size of test specimens (15–29 mg in weight). If we assume that the NRM-lost

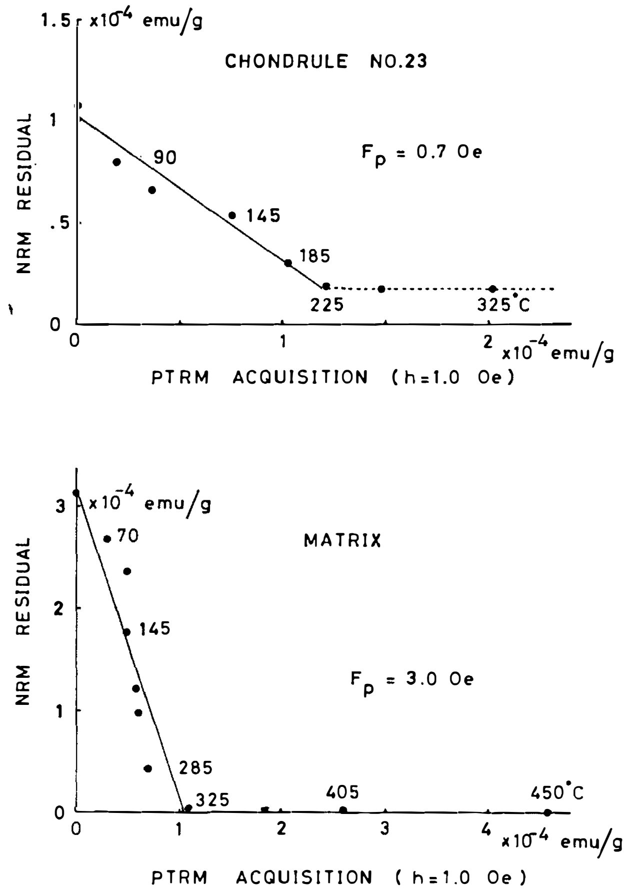

Fig. 19. Königisberger-Thellier plots for an Allende chondrule and a piece of Allende matrix (after SUGIURA *et al., 1979).*

and the PTRM-gained are linearly related in a temperature range below 330°C in the case of matrix too, the F_p-values of matrix can be estimated from data in Fig. 18 as $F_p =$ (2–3) Oe. In Fig. 19, typical examples of the NRM-lost *vs.* PTRM-gained plots of matrix and chondrule of the Allende obtained by SUGIURA *et al.* (1979) are illustrated for comparison. Comparing Fig. 19 (bottom) with Fig. 18, it can be remarked that the NRM-lost *vs.* PTRM-gained plots obtained by SUGIURA *et al.* are very similar to those in the present results, particulary to those of matrix specimens (1) and (2).

Figure 20 shows the NRM-lost *vs.* PTRM-gained plots in the Königisberger-Thellier experiments of the three chondrule specimens, the thermal demagnetization curves of which are shown in Figs. 10 and 11. As already described, (A-2-1) chondrule has the AF- and thermal demagnetization characteristics which are very similar to those of the bulk and matrix specimens. In Fig. 20 also, the NRM-lost *vs.* PTRM-gained plots of (A-2-1) chondrule are not much different from those of the bulk and matrix specimens, though the residual NRM intensity of (A-2-1) chondrule after thermally demagnetizing to 330°C is a little larger than that of the bulk and matrix specimens. From an approximate linear relation between NRM-lost and PTRM-gained in a temperature range below 330°C, the paleointensity of this chondrule can be roughly evaluated to be about 1.3 Oe. The NRM-lost *vs.* PTRM-gained plots for two chondrules

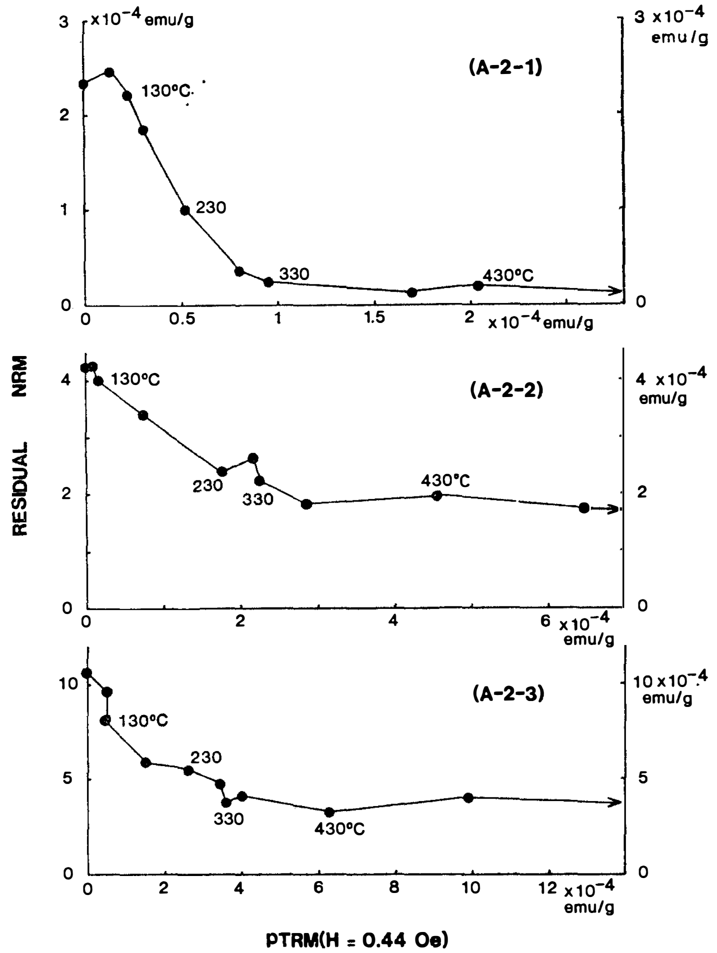

Fig. 20. Königisberger-Thellier plots for 3 Allende chondrules (magnetic field for acquisition of PTRM = 0.44 Oe).

(A-2-2) and (A-2-3) appear to be composed of two components, *i.e.* a component corresponding to a temperature range below 330°C and the other component corresponding to a higher temperature range from 330°C to about 600°C (see Fig. 11 also). Since the larger parts of NRM of these two chondrules were already AF-demagnetized before the Königisberger-Thellier experiments including the thermal demagnetization process, the paleointensity determination technique cannot be applied on these data. A remark worthwhile to be noted will be that the general trend of the NRM-lost *vs.* PTRM-gained plots of these two chondrules looks similar to that of an Allende chondrule examined by SUGIURA *et al.* (1979) (Fig. 19 top).

Summarizing all the experimental results of AF-demagnetization, thermal demagnetization and Königisberger-Thellier experiment of NRMs of bulk specimen, chondrule, and matrix of the Allende chondrite, it may be concluded in the present study that the largest parts of NRM of the Allende are attributable to a stable and uniform NRM of the matrix which disappears at temperatures higher than about 320°C, and that the paleointensity of the bulk and matrix part of the Allende chondrite is estimated as $F_p = (1-3)$ Oe on an assumption that NRM was acquired with the process of PTRM acquisition, through either a hypothesis (a) or another hypothesis (b).

8. Concluding Remarks

In the present study, several points of the magnetic properties and NRM characteristics of the Allende chondrite are confirmed or reconfirmed. These points are as follows:

(1) The ferromagnetic or ferrimagnetic constituents in the Allende are Ni-rich Fe-Ni metal (taenite) of 67–70 wt % Ni, magnetite and ferrimagnetic pyrrhotite (Tables 1, 2 and 3).

(2) The thermomagnetic curve indicates that taenite and/or magnetite is dominant as the ferro- or ferri-magnetism bearer in the Allende (Figs. 2 and 3).

(3) NRM of the bulk specimen of the Allende is reasonably uniform and very stable in the AF-demagnetization test (Figs. 4, 5 and 6, Table 5). NRM of the matrix part also is as stable as that of the bulk specimen (Fig. 7, Table 7).

(4) NRM of the larger number of chondrules is not stable in the AF-demagnetization test or very weak compared with that of matrix, so that the bulk NRM may be mostly represented by that of matrix (Fig. 7, Table 6).

(5) The thermal demagnetization of NRM of the bulk specimen and matrix shows that their NRM is thermally demagnetized almost completely at about 320°C (Figs. 8, 9 and 10). Since the thermal demagnetization curve of these NRMs is very similar to the thermomagnetic curve of ferrimagnetic pyrrhotite (Fig. 12), the ferri- or ferro-magnetic phase bearing the NRM is provisionally called "apparent pyrrhotite" in the present work.

(6) A stable NRM of an Allende chondrule can be attributed to the apparent pyrrhotite (Figs. 7 and 10), but NRMs of other two chondrules look like comprising a component attributable to the apparent pyrrhotite and the other component possessed by taenite and/or magnetite phase (Fig. 11).

(7) Because of the coexistence of taenite and magnetite, the Allende chondrite has capability to acquire TRM of these components, when it is cooled from temperatures higher than about 600°C in the presence of a steady magnetic field (Fig. 14). Therefore, the observed result that the stable NRM of the bulk and matrix of the Allende is attributable to the apparent pyrrhotite may be interpreted as due to a possible special thermal history of the Allende chondrite. If we assume that NRM of the Allende was acquired with the TRM mechanism, a possible thermal history of the Allende will be (a) that there was no magnetic field until the Allende chondrite was cooled to about 320°C and then a magnetic field was produced and maintained during a period while it was further cooled down from 320°C, resulting in an acquisition of PTRM of the apparent pyrrhotite. An alternative hypothesis will be that an accretion and consolidation of random oriented fine grains to the parent mass of the Allende chondrite took place only after these grains were cooled down to about 320°C and PTRM was acquired by the consolidated mass during a further cooling process in the presence of a magnetic field.

A somewhat different hypothetical thermal history of the Allende will be (b) that there was no magnetic field during the cooling process of the accreted and coagulated mass of the Allende chondrite, but there was a magnetic field when it was reheated up to about 320°C by some event and again cooled down. Some other thermal histories

of the Allende also may be possible as discussed later.
(8) Assuming that NRM of the bulk and matrix of the Allende is PTRM of the apparent pyrrhotite phase acquired by cooling from 320°C in a magnetic field (F_p) in the course of their hypothetical thermal history (a) or (b), the F_p-values are estimated using the Königisberger-Thellier method, results showing $F_p=(1\text{–}3)$ Oe (Figs. 6, 15, 16 and 18, Table 8).
(9) As the thermal demagnetization curves of PTRM of the Allende bulk specimens experimentally acquired by cooling from 320°C in a magnetic field in laboratory are satisfactorily conformal with those of NRM (Fig. 17), the experimental conclusion summarized by (8) on an assumption of (7) contains no self-contradiction.

Strictly speaking, however, there still remain several key problems which have not yet been resolved in relation to the NRM characteristics of the Allende, or more generally to its magnetic properties.

SUGIURA *et al.* (1979) concluded their paleomagnetic studies of the Allende chondrules by the following description. "It appears that chondrules have both pre- and post-accretional remanence. Chondrules were magnetized when they were cooled through the Curie temperature while they were suspended in the primitive solar nebula. Later, they were assembled into the Allende meteorite which was heated to 300°C during thermal metamorphism or during accretion. Small chondrules were chemically altered and/or their remanences were largely reset by heating and iron migration during this event. On the other hand, the NRM in large chondrules survived this event. The direction of NRM in large chondrules appear to be random and the paleointensities (2–7) Oe, previously determined from those large chondrule (LANOIX *et al.*, 1978b), probably reflect the fields that were present in the early solar nebula. The fields appear to have varied significantly in space and/or time as recorded in the meteorite themselves in various components". It seems that these investigators do not put much emphasis on what they call post-accretional remanence which can be thermally demagnetized by heating to about 320°C. They simply remarked in their paper, "By Thellier's method, almost linear portions on a magnetization-remaining *vs.* magnetization-acquired plot are found for a chondrule and for a white inclusion below 300°C. The paleointensity values (*ca.* 1 Oe) are in agreement with those determined from the whole rock (BANERJEE and HARGRAVES, 1972; BRECHER and ARRHENIUS, 1974; BUTLER, 1972). These results on Group 3 chondrules indicate that they have partial thermoremanence (or thermochemical remanence) which was acquired when the parent body (Allende) was heated to 300°C at the time of formation or by later thermal metamorphism". Their conclusion is largely based on the experimental results of the paleointensity of Allende chondrules obtained by LANOIX *et al.* (1978a, b). In the experimental works by LANOIX *et al.*, an approximate linear relation between the NRM-lost and PTRM-gained reasonably well holds in a temperature range from 350° to 550°C, at which NRM is thermally demagnetized almost completely, while the NRM-lost *vs.* PTRM-gained plots show some zigzag paths in a temperature range below 350°C, particularly at about 100°C and about 300°C.

In the résumé of magnetic studies on the Allende chondrules by WASILEWSKI and SARALKER (1981), on the other hand, their conclusion has been given as follows: "About 90% of the NRM and 80% of the saturation remanence (SIRM) in the Allende meteorite is thermally demagnetized by 320°C. Therefore, the magnetic sulfides, present in chondrules, the matrix, and possible other intrusions, would appear to be responsible for about 90% of the observed stable NRM in Allende. The NRM in the Allende meteorite is stable during AF-demagnetization, and since the unstable chondrule vectors are therefore not detected, they must be oriented randomly, and respond randomly to AF-demagnetization. A sulfidation event was probably responsible for imparting the stable NRM in the Allende meteorite". This conclusion given by WASILEWSKI and SARALKER seems to be nearly close to a provisional conclusion of the present study, though they dealt mostly with the Allende chondrules while the present study is mostly concerned with the bulk specimen and matrix of the Allende. Since the present study deals mostly with the NRM characteristics of the matrix and the bulk specimen of the Allende in fair detail with some reference to those of chondrules, it will be certain that the NRM characteristics of the matrix parts of the Allende and its whole rock, summarized in the present paper, can be a mutually complementary set of data with those of its chondrules in order to understand the whole aspect of the Allende NRM.

As pointed out by WASILEWSKI and SARALKER (1981), there may be a possibility (c) that a stable NRM of the Allende was acquired by the ferrimagnetic pyrrhotite phase as the chemical remanent magnetization (CRM) or the thermo-chemical remanent magnetization (TCRM) during the process of formation of iron sulfide in the presence of a magnetic field. As summarized by CRAIG and SCOTT (1974), the equilibrium diagram of Fe-S binary system in the neighborhood of composition of Fe_7S_8 is much complicated with troilite, antiferromagnetic pyrrhotite, ferrimagnetic pyrrhotite and pyrite phases. In the ternary system of Fe-Ni-S, the equilibrium diagram around the Fe_7S_8 composition is further complicated. In the relatively simple equilibrium phase diagram of Fe-S system, however, an iron sulfide of chemical composition of Fe_7S_8 (stoichiometric pyrrhotite) is paramagnetic at temperatures above 308°C and has a crystal structure of antiferromagnetic pyrrhotite (hexagonal pyrrhotite) at temperatures above 254°C, whereas it has a ferrimagnetic superlattice structure (monoclinic pyrrhotite) at temperatures below 254°C. Iron sulfides containing sulfer a little more than the stoichiometric Fe_7S_8 (*i.e.* up to Fe_9S_{11}, symthite), consist of untiferromagnetic pyrrhotite and pyrite at temperatures above 254°C, while they comprise ferrimagnetic pyrrhotite and pyrite in a temperature range between 254° and 75°C, and ferrimagnetic pyrrhotite and symthite below 75°C. It seems likely, therefore, that the iron sulfide phase having a chemical composition close to the stoichiometric pyrrhotite can acquire TCRM, if it is very slowly cooled down through 254°C in the presence of a magnetic field. It will be significant in relation to the Allende NRM that the possible acquisition process of TCRM by the pyrrhotite phase is experimentally simulated in the future.

References

BANERJEE, S. K. and HARGRAVES, R. B. (1972): Natural remanent magnetization of carbonaceous chondrites and the magnetic field in the early solar system. Earth Planet. Sci. Lett., **17**, 110–119.

BRECHER, A. and ARRHENIUS, G. (1974): The paleomagnetic record in carbonaceous chondrites; Natural remanence and magnetic properties. J. Geophys. Res., **79**, 2081–2106.

BIN, M. and PAUTHENET, R. (1963): Magnetic anisotropy in pyrrhotite. J. Appl. Phys., **34**, 1161–1162.

BUTLER, R. F. (1972): Natural remanent magnetization and thermomagnetic properties of Allende

meteorite. Earth Planet. Sci. Lett., **17**, 23–70.
CRAIG, J. R. and SCOTT, S. D. (1974): Sulfide phase equibria. Sulfide Mineralogy, Vol. 1, ed. by Mineral. Soc. Am., CS-1–CS-110
CRANGLE, J. and HALLAM, G. C. (1963): The magnetization of face-centered cubic and body-centered cubic iron+nickel alloys. Proc. R. Soc. London, Ser. A, **255**, 119–132.
HAGGERTY, S. E. and MCMAHON, B. M. (1979): Magnetite-sulfide-metal complexes in the Allende meteorite. Proc. Lunar Planet. Sci. Conf. 10th, 851–870.
LANOIX, M., STRANGWAY, D. W. and PEARCE, G. W. (1978a): The primordial magnetic field preserved in chondrules of the Allende meteorite. Geophys. Res. Lett., **5**, 73–76.
LANOIX, M., STRANGWAY, D. W. and PEARCE, G. W. (1978b): Paleointensity determinations from Allende chondrules. Lunar and Planetary Science IX. Houston, Lunar Planet. Inst., 630–632.
NAGATA, T. (1961): Rock Magnetism. Tokyo, Maruzen, 350 p.
NAGATA, T. (1979a): Meteorite magnetism and the early solar system magnetic field. Phys. Earth Planet. Inter., **20**, 324–341.
NAGATA, T. (1979b): Natural remanent magnetization of the fusion crust of meteorites. Mem. Natl Inst. Polar Res., Spec. Issue, **15**, 253–272.
OZIMA, M. and NAGATA, T. (1964): Low temperature treatment as an effective means of "magnetic cleaning" of natural remanent magnetization. J. Geomagn. Geoelectr., **16**, 37–40.
SUGIURA, N., LANOIX, M. and STRANGWAY, D. W. (1979): Magnetic fields of the solar nebula as recorded in chondrules from the Allende meteorite. Phys. Earth Planet. Inter., **20**, 342–349.
TAYLOR, L. A. (1979): Paleointensity determinations at elevated temperatures; Sample preparation technique. Proc. Lunar Planet. Sci. Conf. 10th, 2183–2187.
WASILEWSKI, P. J. and SARALKER, C. (1981): Stable NRM and mineralogy of Allende; Chondrule. Proc. Lunar Planet. Sci. Conf. 12B, 1217–1227.

(*Received July 6, 1983; Revised manuscript received August 5, 1983*)

Appendix: NRM of the Fusion Crust of the Allende Chondrite

It has already been reported that the fusion crust of stony meteorites generally possesses NRM of strong intensity, which is certainly acquired as TRM during a short period while the fusion crust part was heated to a very high temperature and then rapidly cooled in the geomagnetic field when the meteorites entered the earth's atmosphere (*e.g.* NAGATA, 1979b). The Allende chondrite also is widely covered by a fusion crust layer which has strong NRM. As the Allende carbonaceous chondrite has dark black color in general, some test specimens which were taken off from a larger bulk mass of the Allende chondrite without sufficient carefulness often contain small fragments of the fusion crust of dark black color. Obviously, the fusion crust NRM must be completely eliminated for the paleomagnetic studies of this kind of meteorite.

Figure A-1 shows an example of changes in X-, Y- and Z-components of NRM of a bulk sample with a fusion crust layer of the Allende dependent on the amount of fusion crust (in unit of mg) scraped off in non-magnetic space (the right half of diagram) and on the peak field intensity of AF-demagnetization of the pure bulk interior after the fusion crust is completely scraped off (the left half of the diagram). In this case, the specific intensity of NRM of the upper part of fusion crust layer is $(1–2)\times 10^{-3}$ emu/g which is in approximate agreement with the total TRM acquired in a magnetic field of 0.44 Oe (Fig. 14), while the NRM intensity of the uncontaminated interior amounts to 3.5×10^{-4} emu/g which is within a probable range of stable NRM component intensity of the Allende chondrite. As seen in Fig. A-1, the directions of each NRM of the

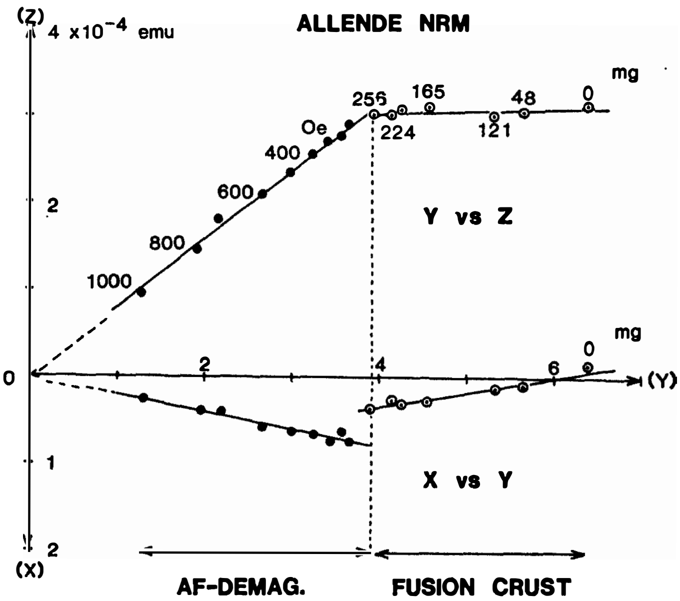

Fig. A-1. *Changes of residual NRM caused by successively scraping off fusion crust layer (right half) and changes of residual NRM of uncontaminated interior by AF-demagnetization (left half) of an Allende bulk sample with a fusion crust layer, projected on (X-Y) and (Y-Z) planes.*

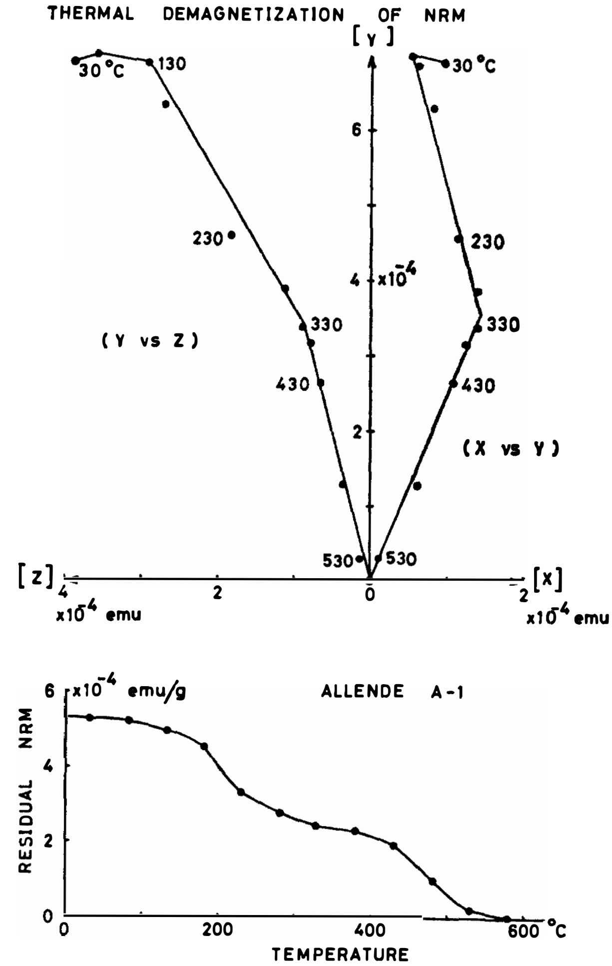

Fig. A-2. *Thermal demagnetization curves of NRM of Allende bulk specimen including small fragments of fusion crust.*
(Top) Projection of residual NRM vectors on (X-Y) and (Y-Z) planes.
(Bottom) Thermal demagnetization curve of NRM intensity.

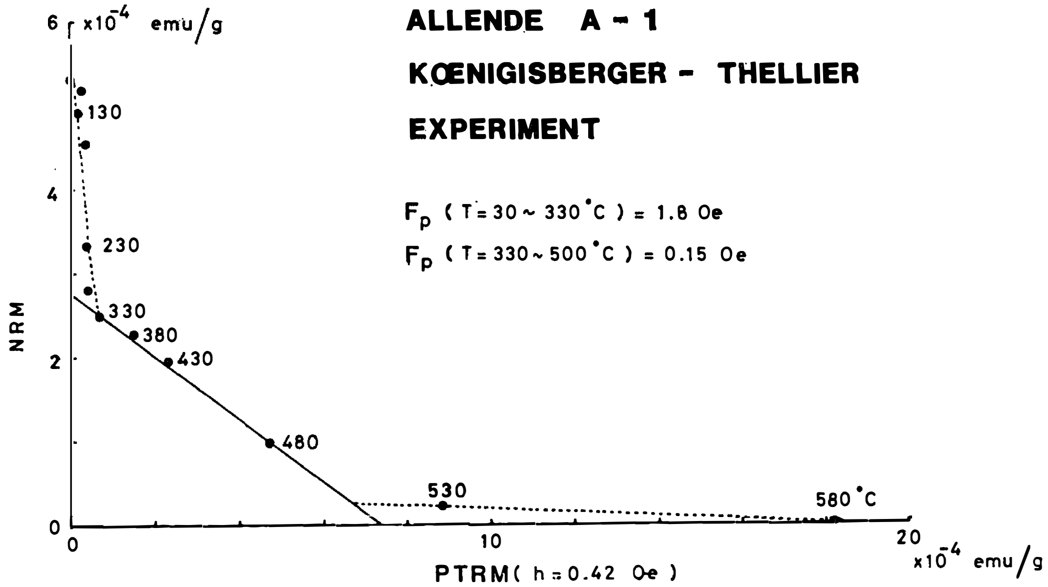

Fig. A-3. Königisberger-Thellier plots for an Allende bulk specimen including small fragments of fusion crust.

fusion crust and the uncontaminated interior are approximately uniform respectively, but these directions are clearly different from each other.

In the course of preparing a number of the Allende bulk specimen for the purpose of their thermal demagnetization of NRM and Königisberger-Thellier experiments, several specimens are still contaminated by samll fragments of the fusion crust. Figure A-2 shows an example of the NRM thermal demagnetization characteristics of such contaminated specimens. It may be obvious in Fig. A-2 that NRM of this bulk specimen consists of 2 components, *i.e.*, a component which can be thermally demagnetized at about 330°C and the other component which can be thermally demagnetized at about 580°C.

The Königisberger-Thellier plots of this specimen are shown in Fig. A-3, where apparent paleointensities of the two components are approximately given as $F_p=1.8$ Oe and $F_p=0.15$ Oe respectively. The NRM component corresponding to $F_p=1.8$ Oe presents NRM possessed by the apparent pyrrhotite which is common in the uncontaminated bulk specimen and the uncontaminated matrix such as shown in Figs. 15, 16 and 18, while the NRM component corresponding to $F_p=0.15$ Oe may represent TRM of the fusion crust fragments which is largely due to the magnetite/taenite phase.